

AD-A254 413



2

PL-TR-92-2110(I)

**DATA TO TEST AND EVALUATE THE PERFORMANCE
OF NEURAL NETWORK ARCHITECTURES FOR
SEISMIC SIGNAL DISCRIMINATION**

**Thomas J. Sereno, Jr.
Gagan B. Patnaik**

**Science Applications International Corporation
10260 Campus Point Drive
San Diego, California 92121**

27 September 1991



Scientific Report No. 1 (Volume I)

APPROVED FOR PUBLIC RELEASE; DISTRIBUTION UNLIMITED



**PHILLIPS LABORATORY
AIR FORCE SYSTEMS COMMAND
HANSCOM AIR FORCE BASE, MASSACHUSETTS 01731-5000**

92-18371



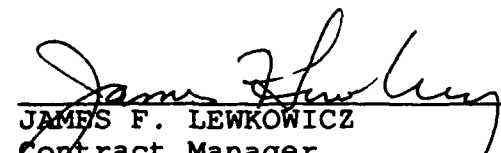
102

SPONSORED BY
Defense Advanced Research Projects Agency
Nuclear Monitoring Research Office
ARPA ORDER NO. 5307

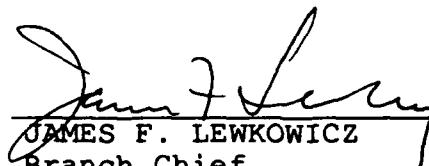
MONITORED BY
Phillips Laboratory
Contract No. F19628-90-C-0156

The views and conclusions contained in this document are those of the authors and should not be interpreted as representing the official policies, either expressed or implied, of the Defense Advanced Research Projects Agency or the U.S. Government.


This technical report has been reviewed and is approved for publication.



JAMES F. LEWKOWICZ
Contract Manager
Solid Earth Geophysics Branch
Earth Sciences Division



JAMES F. LEWKOWICZ
Branch Chief
Solid Earth Geophysics Branch
Earth Sciences Division



DONALD H. ECKHARDT, Director
Earth Sciences Division

This report has been reviewed by the ESD Public Affairs Office (PA) and is releasable to the National Technical Information Service (NTIS).

Qualified requestors may obtain additional copies from the Defense Technical Information Center. All others should apply to the National Technical Information Service.

If your address has changed, or if you wish to be removed from the mailing list, or if the addressee is no longer employed by your organization, please notify PL/IMA, Hanscom AFB, MA 01731-5000. This will assist us in maintaining a current mailing list.

Do not return copies of this report unless contractual obligations or notices on a specific document requires that it be returned.

REPORT DOCUMENTATION PAGE			Form Approved OMB No. 0704-0188	
Public reporting burden for this collection of information is estimated to average 1 hour per response, including the time for reviewing instructions, searching existing data sources, gathering and maintaining the data needed, and completing and reviewing the collection of information. Send comments regarding this burden estimate or any other aspect of this collection of information, including suggestions for reducing this burden, to Washington Headquarters Services, Directorate for Information Operations and Reports, 1215 Jefferson Davis Highway, Suite 1204, Arlington, VA 22202-4302, and to the Office of Management and Budget, Paperwork Reduction Project (0704-0188), Washington, DC 20503				
1. AGENCY USE ONLY (Leave blank)	2. REPORT DATE 27 September 1991	3. REPORT TYPE AND DATES COVERED Scientific Report No. 1 (Volume I)		
4. TITLE AND SUBTITLE Data to Test and Evaluate the Performance of Neural Network Architectures for Seismic Signal Discrimination		5. FUNDING NUMBERS PE 61101E PR 9T10 TA DA WU AA Contract F19628-90-C-0156		
6. AUTHOR(S) Thomas J. Sereno, Jr Gagan B. Patnaik				
7. PERFORMING ORGANIZATION NAME(S) AND ADDRESS(ES) Science Applications International Corporation 10260 Campus Point Drive San Diego, CA 92121		8. PERFORMING ORGANIZATION REPORT NUMBER SAIC-91/1236		
9. SPONSORING/MONITORING AGENCY NAME(S) AND ADDRESS(ES) Phillips Laboratory Hanscom AFB, MA 01731-5000 Contract Manager: James Lewkowicz/GPEH		10. SPONSORING/MONITORING AGENCY REPORT NUMBER PL-TR-92-2110 (I)		
11. SUPPLEMENTARY NOTES				
12a. DISTRIBUTION / AVAILABILITY STATEMENT Approved for public release; Distribution unlimited		12b. DISTRIBUTION CODE		
13. ABSTRACT (Maximum 200 words) This report describes a data set that was developed to test and evaluate the performance of neural networks for automated processing and interpretation of seismic data. This data set may also be valuable for many other studies related to seismic monitoring of nuclear explosion testing at regional distance. It includes waveform and parametric data from 241 regional events recorded by the short-period elements of the NORESS and ARCESS arrays in Norway (33 channels/array). The waveform data are stored in SAC binary format, and the parametric data are stored in ASCII files. The event epicentral distances are 200-1800 km, and the event <i>Lg</i> magnitudes are approximately 1.5-3.2. Most of the events are mining explosions in western USSR, Sweden, and Finland. However, 18 of the events are earthquakes, and 22 are presumed underwater explosions. Detailed documentation has been developed for each event, and is included in eight separate database reports.				
14. SUBJECT TERMS Neural networks Seismic database NORESS/ARCESS		Regional seismology	15. NUMBER OF PAGES 64	16. PRICE CODE
17. SECURITY CLASSIFICATION OF REPORT Unclassified	18. SECURITY CLASSIFICATION OF THIS PAGE Unclassified	19. SECURITY CLASSIFICATION OF ABSTRACT Unclassified	20. LIMITATION OF ABSTRACT SAR	

Table of Contents

1.	INTRODUCTION	1
	1.1 Project Objectives	1
	1.2 Current Status	1
	1.3 Outline of the Report	2
2.	DATA SET #1	3
	2.1 NORESS/ARCESS Arrays	3
	2.2 Regional Events	3
	<i>2.2.1 Selection Criteria</i>	<i>3</i>
	<i>2.2.2 Event Description</i>	<i>8</i>
	2.3 Data Exchange Format	20
	<i>2.3.1 Parametric Data</i>	<i>20</i>
	<i>2.3.2 Waveform Data</i>	<i>22</i>
	<i>2.3.3 Database Reports</i>	<i>25</i>
3.	SUMMARY	35
	ACKNOWLEDGMENTS	35
	REFERENCES	37
	APPENDIX A: PARAMETRIC DATA EXCHANGE FORMAT	39



Accession For	
NTIS GRA&I	<input checked="" type="checkbox"/>
DTIC TAB	<input type="checkbox"/>
Unannounced	<input type="checkbox"/>
Justification	
By _____	
Distribution/	
Availability Codes	
Dist	Avail and/or Special
A-1	

1. INTRODUCTION

1.1 Project Objectives

The objectives of this two-year study are:

- (1) *Assemble three data sets to be used to test and evaluate the performance of neural networks for automated processing and interpretation of seismic data (Table 1).*

Table 1. Seismic Data Sets for the DARPA Neural Network Program

Data Set	Description
<i>Data Set #1</i>	Data from approximately 300 events to develop and train neural networks to perform seismic data processing and interpretation tasks such as automated phase association, onset time estimation, typical and atypical event recognition, and event identification [LaCoss <i>et al.</i> , 1990].
<i>Data Set #2</i>	Data from approximately 30 events to test the response of the neural networks to <i>novelty</i> signals. These data are recorded at the same stations as the events in Data Set #1, but are from different source types.
<i>Data Set #3</i>	Data from approximately 300 events to test the generality and adaptability of the neural networks. These events are recorded by stations in a different geologic environment than the stations used for Data Set #1.

These data sets are to be provided to a group at *MIT* Lincoln Laboratory who is developing and testing neural networks for the seismic application of the DARPA Neural Network Program.

- (2) *Evaluate the results of the neural network program in the context of monitoring nuclear explosion testing.*

1.2 Current Status

Much of our effort during the first year of this project was on the development of Data Set #1. This data set consists of short-period waveforms and parametric data from 241 regional events recorded by the NORESS and ARCESS arrays in Norway. Data Set #1 also includes parametric data from 249 other events (e.g., arrival times, amplitudes, polarization attributes, etc) recorded at NORESS and ARCESS during a continuous 10-day period. The delivery of this data set to *MIT* Lincoln Laboratory was completed in March, 1991 (the total data volume is about 1.2 GBytes). Since their project began several months before ours, we also provided them with 3-

component waveform data recorded by the center element of the NORESS array from 73 regional events that we assembled under a separate DARPA contract. These data were delivered to *MIT* Lincoln Laboratory in March 1990.

We recently began to assemble Data Set #2 which will consist of about 30 earthquakes recorded at NORESS and ARCESS (only 18 of the 241 events in Data Set #1 are earthquakes). We expect to deliver this test data set to *MIT* Lincoln Laboratory in September, 1991. Data Set #3 will probably consist of events recorded by regional arrays in Germany, GERESS, and Finland, FINESA. Data from these arrays are currently being archived at the Center for Seismic Studies (CSS). We will assemble this data set during the second year of our project.

We have several concurrent efforts directed towards the evaluation of neural network techniques in the context of monitoring nuclear explosion testing. First, we plan to integrate the neural network developed by *MIT* Lincoln Laboratory for automated regional phase association into the *Intelligent Monitoring System (IMS)*. *IMS* is a DARPA-sponsored computer system for automated processing and interpretation of seismic data recorded by arrays and single stations [Bache *et al.*, 1990, 1991]. This system has been in operation at CSS since October, 1990 (its predecessor, the *Intelligent Array System*, has been in operation since October, 1989). The neural network developed by *MIT* Lincoln Laboratory assigns a regional phase identification (e.g., P_n , P_g , S_n , L_g , or R_g) to detections registered at array stations. We will integrate this neural network into *IMS*, and compare its performance to that of the current rule-based expert system using data recorded at NORESS and ARCESS. *MIT* Lincoln Laboratory sent us their software module in August, 1991. We are currently testing this module, and we will begin system integration within the next few weeks.

Another important problem in automated seismic data interpretation is initial phase identification (P or S) using data recorded by 3-component stations. We developed neural networks for this application, and trained and tested them on data recorded by the 3-component elements of the NORESS and ARCESS arrays, and on data recorded by the 3-component IRIS stations in the Soviet Union. This effort is described in detail in Volume II of this report [Patnaik and Sereno, 1991b]. We are integrating this neural network into *IMS*, and we will compare its performance to that of the rule-based system using data recorded by the IRIS stations.

1.3 Outline of the Report

This annual report is divided into two separate volumes. Volume I (this document) is a description of Data Set #1 that was provided to *MIT* Lincoln Laboratory for their neural network study. Volume II presents the results of our own neural network application to the problem of initial phase identification using polarization attributes derived from 3-component data [Patnaik and Sereno, 1991b].

The main technical section of Volume I is Section 2. Section 2.1 describes the NORESS and ARCESS arrays and instrumentation. Section 2.2 gives a description of the regional events in Data Set #1 (e.g., location, magnitudes, distances, and identification). The exchange format for waveform and parametric data is described in Section 2.3 and Appendix A. Section 3 summarizes Data Set #1.

2. DATA SET #1

Data Set #1 includes single-channel waveform data, beams, and parametric data from 241 regional events recorded by the NORESS and ARCESS arrays in Norway. The purpose for assembling this data set is to use it to develop and train neural networks to perform seismic data processing and interpretation tasks. However, this data set may also be useful for many other seismic research applications. Data Set #1 is available at SAIC, and the purpose of this report is to describe it in detail.

2.1 NORESS/ARCESS Arrays

The NORESS and ARCESS arrays in Norway include 25 short-period instruments in four concentric rings with a maximum diameter of 3 km (Figure 1). The array configuration and sampling rate were designed to enhance the detection of regional signals [Mykkeltveit, *et al.*, 1983; Mykkeltveit and Ringdal, 1988]. The radius of the inner ring (called the A-ring) is about 150 m. The radii of the B-, C-, and D-rings are 300 m, 700 m, and 1500 m, respectively. The number of sensors on the A-, B-, C-, and D-rings are 3, 5, 7, and 9, respectively. The individual station locations for the NORESS and ARCESS arrays are given in Table 2 (locations are given relative to the reference locations listed at the bottom of this table). Four of the 25 array elements are equipped with 3-component seismometers. These are the center element (A0), and three sensors on the C-ring (C2, C4, and C7). The rest of the array elements only have vertical-component seismometers.

The NORESS and ARCESS data are continuously recorded, and the short-period data are digitized at a rate of 40 samples/s. Figure 2 shows the short-period instrument response. This response applies to all elements of the NORESS and ARCESS arrays. The instrument response is approximately flat to velocity between 2 and 8 Hz. The digitization gain is 10^5 digital counts/volt.

2.2 Regional Events

This section describes the events in Data Set #1. It gives the event locations, magnitudes, epicentral distances from NORESS and ARCESS, and identifications (e.g., explosion or earthquake).

2.2.1 Selection Criteria

Data Set #1 was developed to support the seismic application of DARPA'S Neural Network Program. The goal of this application is determine whether or not neural networks can improve upon current methods for seismic monitoring of nuclear explosion testing. The emphasis is on low yields, so the primary interest is on regional distances ($< 20^\circ$). We used data from NORESS and ARCESS for Data Set #1 because these are prototype arrays for regional monitoring, and there is a large database of waveforms and parametric data archived at CSS. The NORESS and ARCESS data are continuously processed by IMS, and the results of the automated

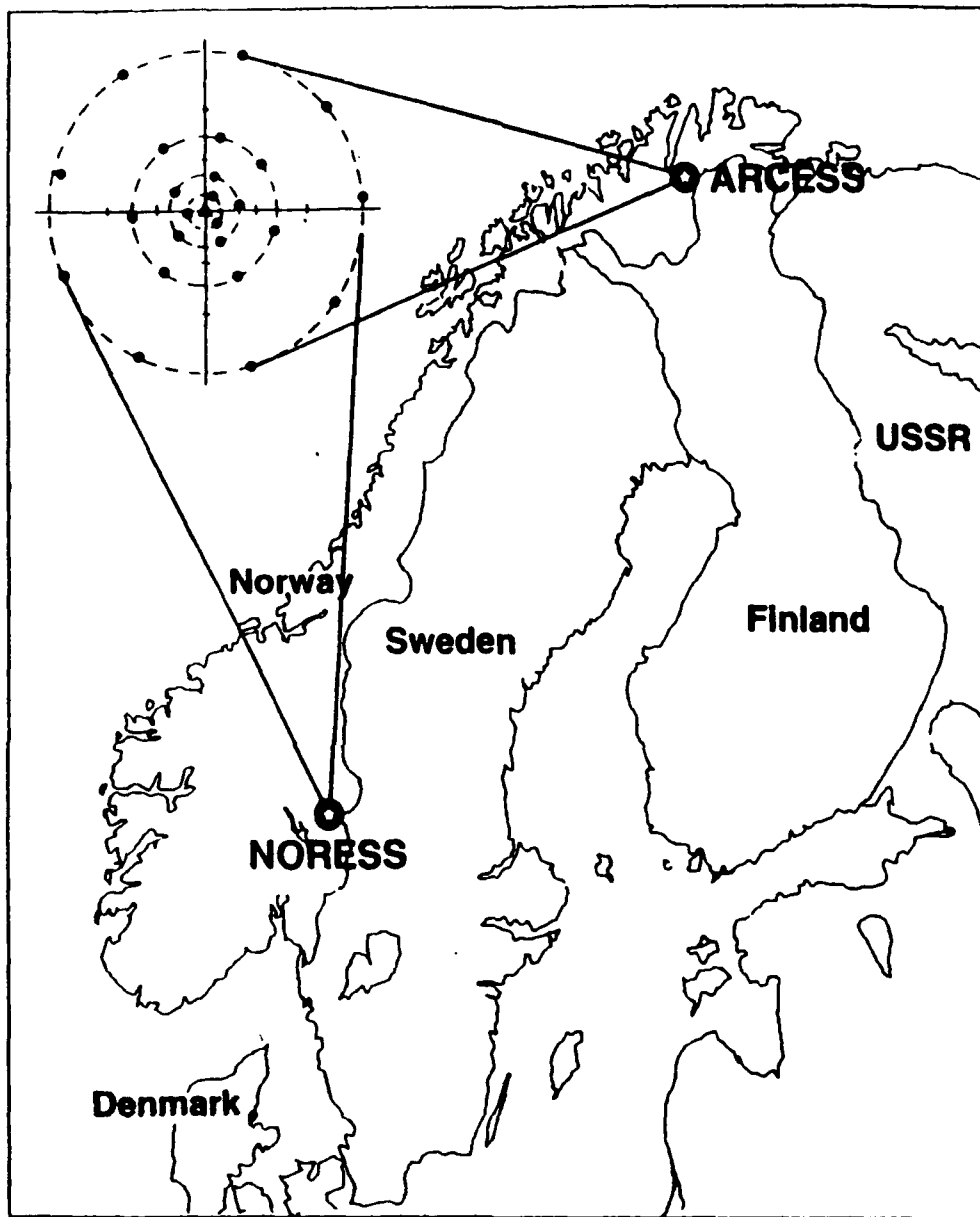


Figure 1. The location and array geometry are plotted for the NORESS and ARCESS arrays (Figure provided by Frode Ringdal, NORSAR).

Table 2. Station Locations

NORESS				ARCESS			
Station	Elevation (km)	dnorth ¹ (km)	deast ¹ (km)	Station	Elevation (km)	dnorth ² (km)	deast ² (km)
NRA0	.3020	.0030	.0040	ARA0	.4030	.0010	-.0003
NRA1	.2910	.1460	.0490	ARA1	.4110	.1600	.0530
NRA2	.3110	-.1030	.1080	ARA2	.3920	-.1210	.0770
NRA3	.2960	-.0300	-.1430	ARA3	.4020	-.0300	-.1490
NRB1	.2990	.3210	.0700	ARB1	.4140	.3360	.0820
NRB2	.3150	.0300	.3340	ARB2	.3970	.0970	.2940
NRB3	.3140	-.2980	.1430	ARB3	.3760	-.2690	.1890
NRB4	.2990	-.2170	-.2280	ARB4	.3780	-.2250	-.2310
NRB5	.2890	.1630	-.2720	ARB5	.4050	.1580	-.2830
NRC1	.2990	.6870	.1090	ARC1	.3810	.6900	.0810
NRC2	.3390	.3410	.6030	ARC2	.3950	.3863	.6657
NRC3	.3520	-.2380	.6470	ARC3	.3760	-.2140	.6730
NRC4	.3110	-.6570	.2080	ARC4	.3770	-.6167	.2287
NRC5	.2990	-.5690	-.3960	ARC5	.3740	-.5380	-.2960
NRC6	.3030	-.0480	-.6870	ARC6	.3950	-.0810	-.6830
NRC7	.2750	.5480	-.4470	ARC7	.3620	.5300	-.4700
NRD1	.3050	1.4800	.1920	ARD1	.3950	1.4910	.1350
NRD2	.3720	1.0150	1.0980	ARD2	.3660	1.1430	.9720
NRD3	.4530	.0760	1.4930	ARD3	.3310	.1880	1.6510
NRD4	.3790	-.9010	1.1890	ARD4	.3710	-.8580	1.1810
NRD5	.3480	-1.4510	.3350	ARD5	.3510	-1.4940	.2330
NRD6	.3520	-1.3260	-.6810	ARD6	.4130	-1.3470	-.6130
NRD7	.3370	-.5660	-1.3680	ARD7	.4130	-.6070	-1.3600
NRD8	.3010	.4140	-1.3360	ARD8	.3680	.3920	-1.4430
NRD9	.2780	1.2570	-.8020	ARD9	.3590	1.1730	-.7780

1. Relative to the reference location: 60.735°N, 11.541°E.
2. Relative to the reference location: 69.535°N, 25.506°E.

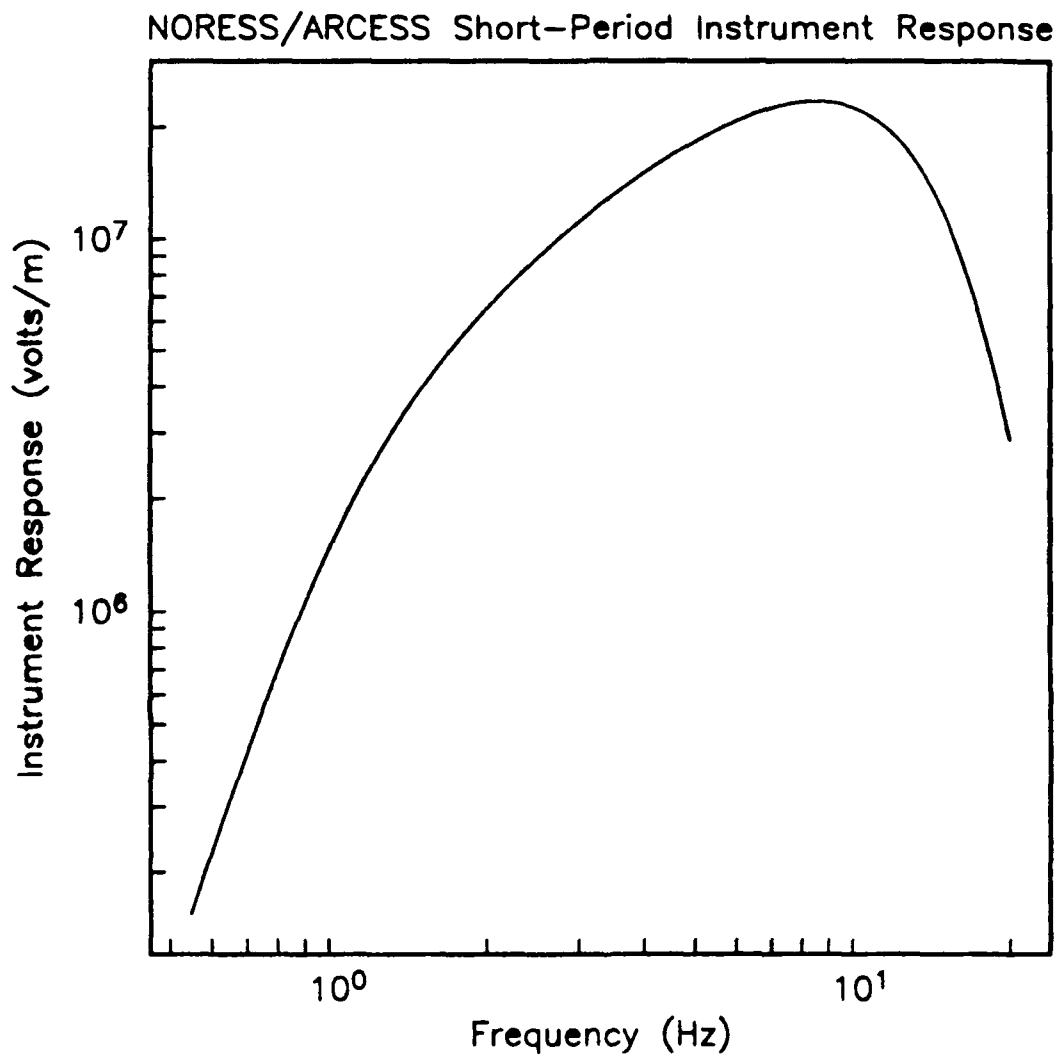


Figure 2. The short-period instrument response is plotted for NORESS and ARCESS.

system are reviewed by seismic analysts. The automated results, the analyst results, and comparisons between them are stored in an on-line relational database at CSS. Thus, these data provide an excellent opportunity to identify deficiencies in the current automated system, and to improve its performance.

MIT Lincoln Laboratory defined several goals for improving the automated monitoring system using neural network techniques. These include regional phase identification, onset time estimation, typical and atypical event detection, and event identification [LaCoss *et al.*, 1990; LaCoss *et al.*, 1991]. Based on these goals, they requested eight separate waveform databases for Data Set #1. These are listed as DB1-DB8 in Table 3. They also requested a separate parametric database (without waveforms) for 10 days of continuous operation. This is listed as DB9 in Table 3.

Table 3. Data Set #1

Database	Description	Number of Events	
		Requested	Provided
DB1	High-Quality Regional Analyst-Corrected	50	50
DB2	High-Quality Regional Analyst-Accepted	50	20
DB3	Random Selection of Analyst-Corrected	50	50
DB4	Random Selection of Analyst-Accepted	50	N/A
DB5	Random Selection of Analyst-Rejected	25	N/A
DB6	Non-event (Noise) Detections	40	N/A
DB7	Teleseisms	25	N/A
DB8	Unusual Events	10	21
DB9	10-days of Parametric Data	N/A	249†
DB10	High-Quality Regional Analyst-Corrected	N/A	50
DB11	High-Quality Regional Analyst-Corrected	N/A	50

† Waveforms were not provided.

Data Set #1 was developed on the basis of this request. It includes waveforms and parametric data from the *Intelligent Array System (IAS)* before and after analyst review (these data are described in the next section). *IAS* was the predecessor to *IMS*. It was specifically designed for the two-array network of NORESS and ARCESS, and it did not attempt to locate teleseismic events. *IMS* currently processes data from a network of four European arrays, and two 3-component stations in Poland (3-component stations in the Soviet Union and China will also be added to this network). *IMS* locates both regional and teleseismic events, and its results are similar to those from *IAS* for events that are at regional distance from either NORESS or ARCESS.

We used data from *IAS* rather than the current *IMS* because *IMS* was not operational until November 1990, which was two months after the start of our contract. Also, the rules used in its knowledge-based system were modified frequently to improve performance until approximately April, 1991. However, results from *IAS* between October, 1989 and October, 1990 are archived at CSS. The only disadvantage of using the *IAS* data is that waveforms were not saved for all events. The criteria for saving waveforms varied slightly over time, but they were based primarily on the

event location, number of detecting stations, and event magnitude. Because waveforms were saved for only selected events, we were not able to satisfy all the requests in DB1-DB8. Therefore, we added two additional databases, DB10 and DB11.

The criteria for selecting events for Data Set #1 varied for each database in Table 3. For all databases, we required event latitudes to be between 50° and 80° , and longitudes to be between -10° and 40° (e.g., regional distance from NORESS or ARCESS). We also required that the waveforms be saved on-line at CSS. For DB1, DB10, and DB11 we require "high-quality" events for which the results of the automated system were corrected in some way by an analyst (e.g., retiming a detection, renaming a phase, etc). We define "high-quality" as events detected at both arrays whose locations are constrained by at least 3 defining phases. In addition, for DB1 we required that all events be detected after January 1, 1990 to ensure that they were reviewed by the same (NORSAR) analyst. This constraint had to be relaxed to get enough events for DB10 and DB11. The same criteria were used for DB3 (random selection of analyst-corrected events) that were used for DB1, except there were no constraints on the number of detecting stations or the number of defining phases (e.g., the "high-quality" constraints).

The original request for DB2 was 50 high-quality events for which the results of the automated system were accepted by an analyst. There are very few of these events with waveforms saved in the IAS database, so we were forced to relax the high-quality constraint. Instead, we provided all analyst-accepted events with waveforms within our latitude and longitude bounds (20 events). Of course, this meant that there were no events to provide as DB4. The request for DB5 was for events that were formed by the automated system, and then rejected by an analyst. There are rejected events in the IAS database, but waveforms are not saved. Therefore, we could not provide DB5. DB6 and DB7 are requests for noise and teleseismic detections, respectively. A detection is labeled "N" for noise by IAS if the phase velocity estimated using a broadband $f-k$ method is less than 2.8 km/s, and it is not associated with an event. Similarly, a detection is labeled "T" for teleseism by IAS if the estimated phase velocity is greater than 14 km/s, and it is not associated with a regional event. Using these definitions, there are 50 "teleseismic" detections and 142 "noise" detections in the other waveform databases in Table 3. However, these labels are based only on the estimate of phase velocity, and they have not been validated by an analyst.

The request for DB8 was for 10 unusual events. For this, we gathered data from multiple-event sequences that include two or more events with origin times that are within 60 s of each other. These events produce mixed signals (e.g., interleaved phases) at either NORESS or ARCESS, or both. This database consists of 21 events in 10 multiple-event sequences. The only other criteria applied to the selection of these data were the latitude and longitude bounds.

2.2.2 Event Description

Table 4 lists the 241 events in Data Set #1 for which waveforms were provided. The first column lists the *orid*, which is a unique positive integer that identifies each event in the CSS database [Anderson *et al.*, 1990]. The second column lists the

Table 4. Events With Waveforms in Data Set #1

orid	Database	Origin Time		Latitude	Longitude	M_L	nsta ¹	ndef ²	Event Type
191531	DB1	90 01 24	16:21:47.014	72.27	-57	2.09	2	3	quake
191546	DB1	90 01 25	05:09:37.277	75.27	25.91	2.39	2	3	quake (H)
191548	DB1	90 01 25	09:49:22.456	68.12	32.83	2.21	2	4	blast (H)
191552	DB1	90 01 25	12:02:30.661	59.47	28.41	2.31	2	5	blast (H)
191571	DB1	90 01 26	10:01:19.878	64.73	30.91	2.23	2	6	blast (H)
191576	DB1	90 01 26	12:04:55.867	59.40	28.58	2.17	2	5	blast (H)
191764	DB1	90 02 02	08:42:06.695	67.70	33.88	2.23	2	7	blast (H)
192008	DB1	90 02 08	14:31:39.935	59.50	26.57	2.32	2	6	blast (H)
191945	DB1	90 02 09	09:32:50.929	67.64	33.72	2.66	2	4	blast (H)
191954	DB1	90 02 09	12:27:59.740	60.96	29.54	2.33	2	4	blast
192093	DB1	90 02 14	10:16:05.013	61.70	31.37	2.19	2	6	blast (H)
192387	DB1	90 02 23	11:16:04.823	61.67	31.72	2.28	2	6	blast (H)
192390	DB1	90 02 23	12:05:06.429	61.13	29.10	2.89	2	5	blast (H)
192671	DB1	90 03 05	12:42:08.275	55.11	30.75	2.31	2	5	expl
192763	DB1	90 03 12	14:34:31.648	60.58	29.60	2.46	2	5	blast (H)
193041	DB1	90 03 23	12:01:52.778	59.31	28.72	2.19	2	6	blast (H)
193078	DB1	90 03 24	15:28:54.658	72.51	4.82	2.62	2	4	quake (H)
193185	DB1	90 03 28	22:21:05.640	54.39	13.73	2.58	2	5	quake
193279	DB1	90 04 02	13:41:10.653	54.40	19.69	2.02	2	4	expl
197468	DB1	90 04 09	08:52:31.104	59.32	28.30	2.05	2	4	blast (H)
197474	DB1	90 04 09	13:02:30.367	59.69	24.98	1.84	2	4	blast (H)
197517	DB1	90 04 11	10:21:17.110	59.20	25.30	2.14	2	6	blast (H)
197522	DB1	90 04 11	11:00:23.168	59.25	28.01	2.45	2	6	blast (H)
197535	DB1	90 04 11	12:48:42.043	69.35	35.41	2.37	2	6	blast (H)
197538	DB1	90 04 11	13:46:06.790	60.83	29.37	2.45	2	5	blast (H)
197576	DB1	90 04 12	11:03:37.894	63.08	28.13	1.89	2	6	blast (H)
197579	DB1	90 04 12	12:09:06.463	69.21	35.28	2.78	2	5	blast (H)
197628	DB1	90 04 14	10:35:18.945	68.11	32.79	2.22	2	4	blast
197712	DB1	90 04 19	11:26:55.068	57.23	11.74	1.24	2	4	expl
197742	DB1	90 04 20	08:57:45.452	54.67	19.72	2.51	2	4	expl
197762	DB1	90 04 20	12:23:40.040	59.82	28.69	2.32	2	4	blast (H)
197764	DB1	90 04 20	13:29:55.864	61.87	30.98	2.36	2	5	blast (H)
197765	DB1	90 04 20	13:56:21.070	61.41	35.35	2.38	2	6	blast
197868	DB1	90 05 02	10:29:15.125	55.54	15.82	2.13	2	3	expl
198004	DB1	90 05 09	16:25:44.411	57.28	7.98	2.08	2	3	expl
198020	DB1	90 05 10	11:31:02.907	62.53	18.32	1.67	2	7	expl
198023	DB1	90 05 10	11:53:46.825	68.02	32.99	2.16	2	4	blast (H)
198052	DB1	90 05 11	17:06:24.382	65.84	25.37	1.42	2	5	blast (H)
198053	DB1	90 05 11	17:07:24.053	67.57	32.90	1.64	2	4	blast (H)
198143	DB1	90 05 15	13:14:50.488	59.37	28.67	2.33	2	6	blast (H)
198261	DB1	90 05 19	20:40:12.834	67.63	34.05	2.37	2	7	blast (H)
198271	DB1	90 05 20	10:23:37.742	55.94	16.27	2.13	2	4	expl
198303	DB1	90 05 21	11:30:47.309	58.74	18.81	2.54	2	6	expl
198384	DB1	90 05 22	09:39:22.879	59.57	22.60	1.43	2	6	blast
198447	DB1	90 05 23	13:37:47.510	69.29	34.85	2.34	2	5	blast (H)
198461	DB1	90 05 23	18:55:26.452	58.16	10.56	1.99	2	3	expl
198462	DB1	90 05 23	19:09:30.078	58.20	10.50	1.00	2	3	expl
198523	DB1	90 05 26	10:06:59.051	68.10	33.79	2.10	2	5	blast (H)
198526	DB1	90 05 26	11:13:00.712	67.62	30.96	2.23	2	6	blast (H)
198546	DB1	90 05 27	21:49:30.059	74.54	9.59	3.21	2	4	quake (H)
103776	DB2	89 10 03	12:29:34.655	63.67	24.92	1.64	2	3	expl

orid	Database	Origin Time		Latitude	Longitude	M_L	nsta ¹	ndef ²	Event Type
105012	DB2	89 10 04	12:20:54.732	69.24	30.51	1.92	1	2	blast (H)
105364	DB2	89 10 04	19:19:44.234	69.12	30.23	.38	1	2	blast
117198	DB2	89 10 12	11:36:51.780	61.44	30.77	2.41	2	3	blast (H)
118906	DB2	89 10 13	11:25:12.799	77.70	33.39	2.62	1	2	quake
177958	DB2	89 11 21	12:54:42.373	59.67	11.53	.42	1	2	expl
184121	DB2	89 11 24	13:01:27.445	59.50	10.26	.96	1	2	expl
191018	DB2	90 01 07	06:25:03.393	67.62	34.05	.00	2	4	blast (H)
191049	DB2	90 01 11	10:10:01.214	59.50	27.77	.00	2	4	blast
191654	DB2	90 02 02	12:58:12.990	61.21	29.79	2.58	2	6	blast (H)
191749	DB2	90 02 07	07:54:16.686	68.59	25.69	.00	1	2	-
192034	DB2	90 02 15	09:48:04.238	67.98	32.96	.00	1	2	blast
192660	DB2	90 03 11	14:14:32.868	75.31	13.47	.00	2	3	quake
192764	DB2	90 03 14	13:06:13.586	59.59	10.07	.00	1	2	expl
193038	DB2	90 03 23	10:12:38.438	59.11	28.26	2.50	2	3	blast (H)
193094	DB2	90 03 27	13:27:03.441	78.49	9.56	2.58	1	2	quake
197366	DB2	90 04 07	05:23:43.882	76.86	25.05	2.27	1	2	quake (H)
198311	DB2	90 05 23	19:04:24.003	67.74	33.69	1.81	1	2	blast (H)
200143	DB2	90 06 01	12:01:24.068	67.34	34.13	2.15	1	2	blast (H)
200149	DB2	90 06 01	18:30:10.651	67.66	33.50	2.08	1	2	blast (H)
191520	DB3	90 01 24	12:01:54.714	59.64	28.33	2.33	2	6	blast
191526	DB3	90 01 24	12:56:48.450	61.32	28.91	2.54	2	3	blast (H)
191527	DB3	90 01 24	13:31:56.883	61.54	32.24	2.60	2	5	blast (H)
191583	DB3	90 01 26	16:22:03.849	75.10	23.41	1.94	1	2	quake
191670	DB3	90 01 30	12:02:20.415	59.27	28.45	2.32	2	5	blast (H)
191806	DB3	90 02 04	01:38:32.574	61.11	26.55	2.52	2	6	quake
191911	DB3	90 02 08	11:31:13.041	59.33	27.24	2.39	2	6	blast (H)
191955	DB3	90 02 09	12:34:47.835	64.78	30.87	2.14	2	6	blast (H)
191987	DB3	90 02 13	11:24:56.765	59.42	27.13	2.34	2	5	blast (H)
192192	DB3	90 02 16	11:34:27.670	59.31	27.98	2.40	2	5	blast (H)
192193	DB3	90 02 16	11:38:47.495	59.37	27.34	2.47	2	5	blast (H)
192199	DB3	90 02 16	12:38:15.632	67.65	34.16	2.81	2	7	blast (H)
192202	DB3	90 02 16	12:55:04.285	60.92	29.47	2.51	2	6	blast (H)
192380	DB3	90 02 23	09:31:22.220	67.64	34.35	2.92	2	7	blast (H)
192436	DB3	90 02 24	19:37:18.179	58.87	18.33	2.93	2	5	expl
192482	DB3	90 02 26	20:30:15.658	57.51	7.27	3.06	2	6	quake (H)
192535	DB3	90 02 28	13:30:42.498	61.11	29.05	2.37	2	6	blast
192554	DB3	90 03 01	09:47:28.040	59.42	27.88	2.31	2	6	blast (H)
192585	DB3	90 03 02	11:01:56.012	67.64	34.08	2.45	2	5	blast (H)
192587	DB3	90 03 02	12:00:23.017	61.12	29.20	2.34	2	6	blast
192452	DB3	90 03 06	10:47:54.178	59.45	27.92	2.21	2	5	blast (H)
192454	DB3	90 03 06	11:32:58.664	59.49	27.25	2.39	2	6	blast (H)
192692	DB3	90 03 07	10:24:51.491	67.61	34.03	3.20	1	3	blast (H)
192791	DB3	90 03 14	08:51:32.961	59.56	35.93	2.03	1	2	-
192864	DB3	90 03 15	11:54:23.370	59.18	27.24	2.52	2	6	blast (H)
192887	DB3	90 03 16	10:33:27.409	67.64	35.02	2.90	1	3	blast (H)
192926	DB3	90 03 20	13:36:59.973	59.23	26.94	2.03	2	6	blast (H)
192969	DB3	90 03 21	14:15:54.343	61.34	35.17	2.33	1	3	blast (H)
193024	DB3	90 03 22	13:21:51.699	60.88	29.10	2.39	2	6	blast
193034	DB3	90 03 23	08:30:23.057	67.60	33.91	2.70	2	7	blast (H)
193156	DB3	90 03 28	10:59:13.988	59.55	27.99	2.19	2	6	blast (H)
193166	DB3	90 03 28	12:00:05.599	59.14	26.89	2.38	2	5	blast (H)
193187	DB3	90 03 29	04:11:18.667	62.07	6.06	2.30	2	7	quake
193201	DB3	90 03 29	11:27:18.825	59.28	27.95	2.37	2	5	blast (H)

orid	Database	Origin Time		Latitude	Longitude	M_L	nsta ¹	ndef ²	Event Type
193203	DB3	90 03 29	11:31:43.507	61.11	29.97	2.75	2	6	blast
193218	DB3	90 03 30	08:49:01.642	67.64	34.11	2.59	2	6	blast (H)
193222	DB3	90 03 30	10:39:03.617	59.24	27.27	2.23	2	6	blast (H)
193250	DB3	90 03 31	14:15:03.805	61.74	30.80	2.51	2	6	blast
193255	DB3	90 04 01	05:06:31.114	67.56	34.20	2.39	2	7	blast (H)
193266	DB3	90 04 02	09:57:29.106	61.13	30.74	2.12	2	4	blast (H)
193270	DB3	90 04 02	10:31:55.798	61.19	30.72	1.90	2	5	blast
193280	DB3	90 04 02	13:46:23.256	52.86	-4.77	2.61	2	4	quake
193281	DB3	90 04 02	14:03:34.589	54.34	19.77	2.12	2	4	expl
197381	DB3	90 04 03	14:16:33.314	58.28	19.06	1.45	2	3	expl
197382	DB3	90 04 03	14:24:33.159	58.38	19.25	2.61	2	5	expl
197408	DB3	90 04 06	09:45:33.118	59.38	27.44	1.91	2	4	blast (H)
197412	DB3	90 04 06	10:36:01.684	60.01	33.62	2.70	2	3	expl
197413	DB3	90 04 06	10:37:02.280	60.97	29.30	2.45	2	5	blast
197417	DB3	90 04 06	11:34:29.834	67.79	34.31	1.96	1	2	blast (H)
197432	DB3	90 04 06	12:20:36.430	64.72	30.85	2.09	2	5	blast (H)
106759	DB8	89 10 04	10:12:40.564	54.71	19.04	2.34	2	3	expl
106762	DB8	89 10 04	10:13:40.029	54.61	19.80	2.43	2	3	expl
118427	DB8	89 10 11	06:22:29.539	58.44	18.72	2.51	2	3	expl
118499	DB8	89 10 11	06:23:18.152	59.19	18.65	2.46	2	3	expl
131912	DB8	89 10 20	14:55:52.442	70.04	23.62	.00	1	2	expl
131916	DB8	89 10 20	14:55:54.385	70.10	23.56	.00	1	2	expl
131917	DB8	89 10 20	14:56:01.685	69.99	23.49	.00	1	2	expl
152005	DB8	89 11 02	23:33:18.495	67.79	20.93	1.07	1	2	blast
152009	DB8	89 11 02	23:33:23.372	67.82	20.86	1.13	1	2	blast
189277	DB8	89 11 21	11:03:29.729	58.62	18.66	2.36	2	4	expl
189330	DB8	89 11 21	11:03:57.490	58.68	18.55	2.36	1	3	expl
197533	DB8	90 04 11	12:38:07.117	55.72	32.60	2.24	2	4	expl
197534	DB8	90 04 11	12:39:15.714	54.20	30.95	2.09	2	5	expl
197593	DB8	90 04 13	10:18:56.028	59.24	27.84	2.35	2	6	blast (H)
197594	DB8	90 04 13	10:19:41.850	67.16	33.06	.77	1	2	blast
197601	DB8	90 04 13	12:58:01.935	67.63	33.45	2.13	2	5	blast (H)
197602	DB8	90 04 13	12:59:18.645	67.63	33.91	1.15	2	4	blast (H)
197704	DB8	90 04 19	09:58:53.558	59.27	27.95	2.02	2	4	blast (H)
197706	DB8	90 04 19	10:00:42.828	59.28	27.64	2.29	2	4	blast (H)
197818	DB8	90 04 28	11:01:07.889	59.39	28.32	1.97	2	5	blast (H)
197819	DB8	90 04 28	11:02:11.118	59.21	27.99	2.14	2	6	blast (H)
103539	DB10	89 10 02	15:11:30.828	59.40	26.93	2.90	2	6	blast (H)
118708	DB10	89 10 11	07:49:36.455	59.81	21.86	2.57	2	6	blast
119051	DB10	89 10 11	10:03:05.858	64.73	30.92	2.56	2	6	blast (H)
123686	DB10	89 10 12	12:20:51.001	61.54	34.63	2.42	2	4	blast (H)
123713	DB10	89 10 12	14:29:28.606	58.06	19.26	2.26	2	4	expl
123721	DB10	89 10 13	11:41:30.794	67.68	33.56	2.77	2	4	blast (H)
123728	DB10	89 10 13	12:00:25.894	64.83	30.50	2.49	2	6	blast (H)
125589	DB10	89 10 16	10:21:15.181	59.29	27.28	2.62	2	6	blast (H)
125900	DB10	89 10 16	12:44:02.741	69.41	30.99	2.62	2	5	blast (H)
127401	DB10	89 10 17	15:00:47.687	59.37	25.20	2.01	2	6	blast (H)
128464	DB10	89 10 17	20:42:08.973	64.95	9.32	2.78	2	4	quake (H)
131862	DB10	89 10 20	06:41:23.940	67.66	34.18	2.84	2	7	blast (H)
131911	DB10	89 10 20	13:25:32.576	59.41	25.22	2.38	2	5	blast (H)
134678	DB10	89 10 24	15:10:35.164	59.55	26.47	2.54	2	6	blast (H)
134688	DB10	89 10 24	18:05:03.191	54.90	20.46	2.17	2	4	expl
135510	DB10	89 10 26	09:24:12.089	57.82	11.69	2.16	2	5	expl

orid	Database	Origin Time		Latitude	Longitude	M_L	nsta ¹	ndef ²	Event Type
135514	DB10	89 10 26	10:13:57.858	61.19	29.97	2.46	2	6	blast (H)
140720	DB10	89 10 26	13:50:58.974	60.54	29.63	2.42	2	6	blast (H)
140725	DB10	89 10 26	14:38:21.700	61.56	31.54	2.42	2	6	blast (H)
140759	DB10	89 10 27	11:32:57.358	64.81	30.43	2.36	2	6	blast (H)
140775	DB10	89 10 27	12:50:43.185	69.45	30.88	2.65	2	6	blast (H)
140819	DB10	89 10 28	11:42:52.921	61.85	36.33	2.58	2	6	blast
147829	DB10	89 11 01	12:25:41.306	59.16	28.09	2.66	2	6	blast (H)
147845	DB10	89 11 01	13:02:59.129	60.93	28.98	2.57	2	6	blast (H)
147846	DB10	89 11 01	13:26:10.027	60.88	29.34	2.68	2	5	blast
147858	DB10	89 11 01	15:59:34.987	61.90	30.79	2.54	2	6	blast (H)
152019	DB10	89 11 03	08:19:34.973	67.68	34.32	2.87	2	7	blast (H)
152059	DB10	89 11 03	13:20:49.061	61.60	25.29	2.35	2	5	blast
152097	DB10	89 11 04	07:39:08.699	67.89	32.30	2.28	2	5	blast
152109	DB10	89 11 04	10:05:21.280	64.78	30.44	2.70	2	6	blast (H)
152944	DB10	89 11 04	12:46:30.901	69.36	30.97	3.03	2	5	blast (H)
152996	DB10	89 11 05	11:05:54.398	59.45	27.11	2.22	2	6	blast (H)
153019	DB10	89 11 06	05:58:40.963	67.68	33.56	2.77	2	7	blast (H)
153033	DB10	89 11 06	11:59:14.428	63.09	28.24	2.26	2	6	blast (H)
155511	DB10	89 11 08	22:56:30.837	67.19	20.96	2.27	2	5	blast (H)
160154	DB10	89 11 09	13:28:18.765	59.32	25.21	2.30	2	5	blast (H)
161012	DB10	89 11 09	14:12:21.951	60.59	29.17	2.49	2	5	blast (H)
160940	DB10	89 11 10	07:06:14.404	65.03	26.41	2.02	2	6	quake (H)
160944	DB10	89 11 10	10:42:14.172	59.43	27.27	2.38	2	6	blast (H)
161037	DB10	89 11 10	12:03:11.747	69.43	30.93	2.25	2	4	blast (H)
160949	DB10	89 11 10	12:40:38.302	54.96	16.40	2.46	2	5	expl
161041	DB10	89 11 10	13:43:38.951	59.58	25.36	2.12	2	4	blast (H)
161317	DB10	89 11 11	07:10:27.217	67.63	33.56	2.17	2	6	blast (H)
161049	DB10	89 11 11	08:41:27.120	67.64	33.97	2.52	2	7	blast (H)
172081	DB10	89 11 14	12:00:33.595	61.17	30.06	2.29	2	4	blast (H)
172095	DB10	89 11 14	14:47:22.230	59.48	26.50	2.76	2	6	blast (H)
172363	DB10	89 11 15	12:08:12.985	63.29	27.74	2.15	2	6	blast (H)
175063	DB10	89 11 16	12:35:06.559	58.93	18.71	2.04	2	5	expl
175305	DB10	89 11 16	14:55:49.832	59.53	27.14	2.24	2	5	blast (H)
177371	DB10	89 11 17	11:00:01.966	64.80	30.72	2.08	2	6	blast (H)
107824	DB11	89 09 29	08:23:16.393	67.53	33.58	2.61	2	5	blast (H)
107849	DB11	89 09 29	12:02:26.738	60.97	29.31	2.87	2	6	blast (H)
107883	DB11	89 09 29	12:30:30.804	61.32	28.77	2.42	2	6	blast (H)
107888	DB11	89 09 29	12:54:34.980	69.40	30.86	2.26	2	3	blast (H)
107890	DB11	89 09 29	13:00:00.756	59.47	26.80	2.54	2	6	blast (H)
107914	DB11	89 09 29	14:13:34.956	59.53	24.96	2.30	2	4	blast (H)
108561	DB11	89 09 30	13:10:08.696	67.63	29.84	2.49	2	4	blast (H)
105219	DB11	89 10 03	11:56:42.915	64.16	23.67	2.15	2	4	expl
106770	DB11	89 10 04	11:27:41.636	61.58	30.33	2.29	2	5	blast (H)
106780	DB11	89 10 04	13:16:20.806	55.79	16.75	2.30	2	4	expl
107868	DB11	89 10 05	11:49:15.124	59.46	23.86	2.17	2	4	blast
108213	DB11	89 10 05	14:48:27.340	59.59	26.47	2.54	2	6	blast (H)
111577	DB11	89 10 06	09:05:55.448	67.59	35.01	2.71	2	4	blast (H)
111585	DB11	89 10 06	10:16:39.153	64.77	31.20	2.44	2	5	blast (H)
111787	DB11	89 10 06	11:12:39.704	59.43	27.13	2.71	2	6	blast (H)
111946	DB11	89 10 06	11:42:14.650	67.64	29.85	2.26	2	3	blast (H)
112156	DB11	89 10 06	12:01:19.638	63.24	27.59	2.12	2	7	blast (H)
115620	DB11	89 10 09	16:20:14.188	67.08	21.24	2.02	2	4	blast (H)
116470	DB11	89 10 10	13:25:58.927	59.02	25.52	2.81	2	5	blast (H)

orid	Database	Origin Time		Latitude	Longitude	M_L	nsta ¹	ndef ²	Event Type
190865	DB11	89 10 17	14:55:04.120	59.55	26.78	2.56	2	5	blast (H)
133590	DB11	89 10 23	13:28:47.537	61.85	31.12	2.44	2	6	blast (H)
140713	DB11	89 10 26	12:59:05.936	59.67	28.22	2.26	2	5	blast (H)
140826	DB11	89 10 27	15:10:30.505	67.72	33.83	2.12	2	4	blast (H)
190881	DB11	89 11 16	13:17:56.963	61.10	29.06	2.33	2	4	blast (H)
177383	DB11	89 11 17	08:24:54.337	67.67	34.15	2.75	2	7	blast (H)
177438	DB11	89 11 18	11:26:46.268	61.86	30.83	2.59	2	6	blast (H)
178839	DB11	89 11 20	12:57:57.410	59.40	27.07	2.24	2	5	blast (H)
189367	DB11	89 11 21	13:05:42.979	61.27	29.78	2.28	2	6	blast (H)
189479	DB11	89 11 24	10:00:34.632	64.84	30.67	2.33	2	4	blast (H)
189461	DB11	89 11 24	12:04:08.162	67.63	34.10	2.91	2	7	blast
189469	DB11	89 11 24	16:02:09.780	66.95	21.66	2.35	2	5	blast (H)
189655	DB11	89 11 25	11:11:45.657	68.07	33.52	2.27	2	7	blast (H)
189658	DB11	89 11 25	12:37:40.038	67.62	30.20	2.37	2	5	blast (H)
192440	DB11	90 02 25	10:00:26.090	59.50	6.83	2.29	2	5	quake (H)
197524	DB11	90 04 11	11:13:08.723	59.17	27.37	2.29	2	6	blast (H)
197580	DB11	90 04 12	12:12:15.582	61.02	28.98	2.18	2	5	blast (H)
197596	DB11	90 04 13	10:47:07.274	58.80	28.33	2.33	2	4	blast
197639	DB11	90 04 14	15:15:22.056	70.02	34.43	2.08	2	6	expl
197671	DB11	90 04 18	10:12:54.031	59.29	27.89	2.03	2	6	blast (H)
197674	DB11	90 04 18	11:39:32.142	59.02	27.74	2.39	2	4	blast (H)
197700	DB11	90 04 19	08:05:27.018	69.16	34.64	2.45	2	6	blast (H)
197741	DB11	90 04 20	08:38:51.774	67.61	33.73	2.51	2	7	blast (H)
197747	DB11	90 04 20	09:57:37.358	58.90	27.16	2.32	2	6	blast (H)
197820	DB11	90 04 28	12:02:02.118	67.98	33.76	2.03	2	5	blast (H)
197825	DB11	90 04 28	14:37:06.044	59.51	26.46	2.23	2	6	blast (H)
197876	DB11	90 05 02	12:05:59.365	57.74	11.72	3.83	2	4	expl
198017	DB11	90 05 10	11:02:46.221	59.33	27.22	2.29	2	6	blast (H)
198039	DB11	90 05 11	11:11:46.391	59.29	27.80	2.33	2	5	blast
198272	DB11	90 05 20	10:27:07.366	68.04	10.95	2.80	2	5	quake (H)
198353	DB11	90 05 21	12:50:39.845	58.30	28.11	2.39	2	4	blast

1. The number of detecting stations.

2. The number of defining phases (number of phases used to locate the event).

database name from Table 3. The rest of the columns list the event origin time, latitude, longitude, L_g magnitude (M_L), number of detecting stations, number of defining phases, and event type. Events that were identified in a regional bulletin produced by the University of Helsinki are indicated by "(H)" following the event type in Table 4. Other events were identified by *Sereno* [1991].

The event locations are plotted in Figure 3. Of the 241 events, 215 were recorded at both NORESS and ARCESS, and 221 had at least 3 defining phases. The epicentral distances are primarily between 200 and 1800 km (Figure 4). The L_g magnitude distribution is plotted in Figure 5. This magnitude is computed from the peak amplitude on a 2–4 Hz incoherent beam in the time window defined by group velocities of 3.0 and 3.6 km/s [*Bache et al.*, 1991]. The magnitudes of the events in Data Set #1 are primarily between 1.5 and 3.2.

Most of the events in Data Set #1 were identified (mine blast or earthquake) in the regional bulletin produced by the University of Helsinki. The other events were either not identified by the University of Helsinki, or they were not in their bulletin. In either case, these events were identified by *Sereno* [1991] on the basis of location, origin time, S/P amplitude ratios, spectral variance, and past seismicity. Along with the identification of each of these events, *Sereno* [1991] gives a brief description of the basis for the identification and a subjective measure of confidence (high, medium, or low). Table 5 lists the number of earthquakes, mine blasts, underwater explosions, and other explosions for each of the waveform databases in Table 3. Events that are probable explosions and are located onshore (but not near known mines) are labeled "other explosions."

Table 5. Event Identification for Data Set #1

Event Type	Number of Events						Total
	DB1	DB2	DB3	DB8	DB10	DB11	
Earthquakes	5	4	5	0	2	2	18
Mine Blasts	34	11	39	10	43	44	181
Underwater Explosions	8	1	3	4	3	3	22
Other Explosions	3	3	2	7	2	1	18
Not Identified	0	1	1	0	0	0	2
Total	50	20	50	21	50	50	241

Figure 6 shows the locations of the presumed earthquakes, mine blasts, and other explosions (either underwater or onshore). Most of the earthquakes are located on the Mid-Atlantic Ridge, or near the west coast of Norway. The mine blasts are primarily in the northwestern USSR (e.g., Estonia, Leningrad, Kola Peninsula), northern Sweden, and Finland. Most of the underwater explosions are located in the Baltic Sea.

The locations of the 249 events in DB9 are shown in Figure 7. These events were recorded over a continuous 10-day period starting February 28, 1990. Data Set #1 does not include waveform data for these events, and the parametric data are described in the next section.

Events With Waveforms in Data Set #1

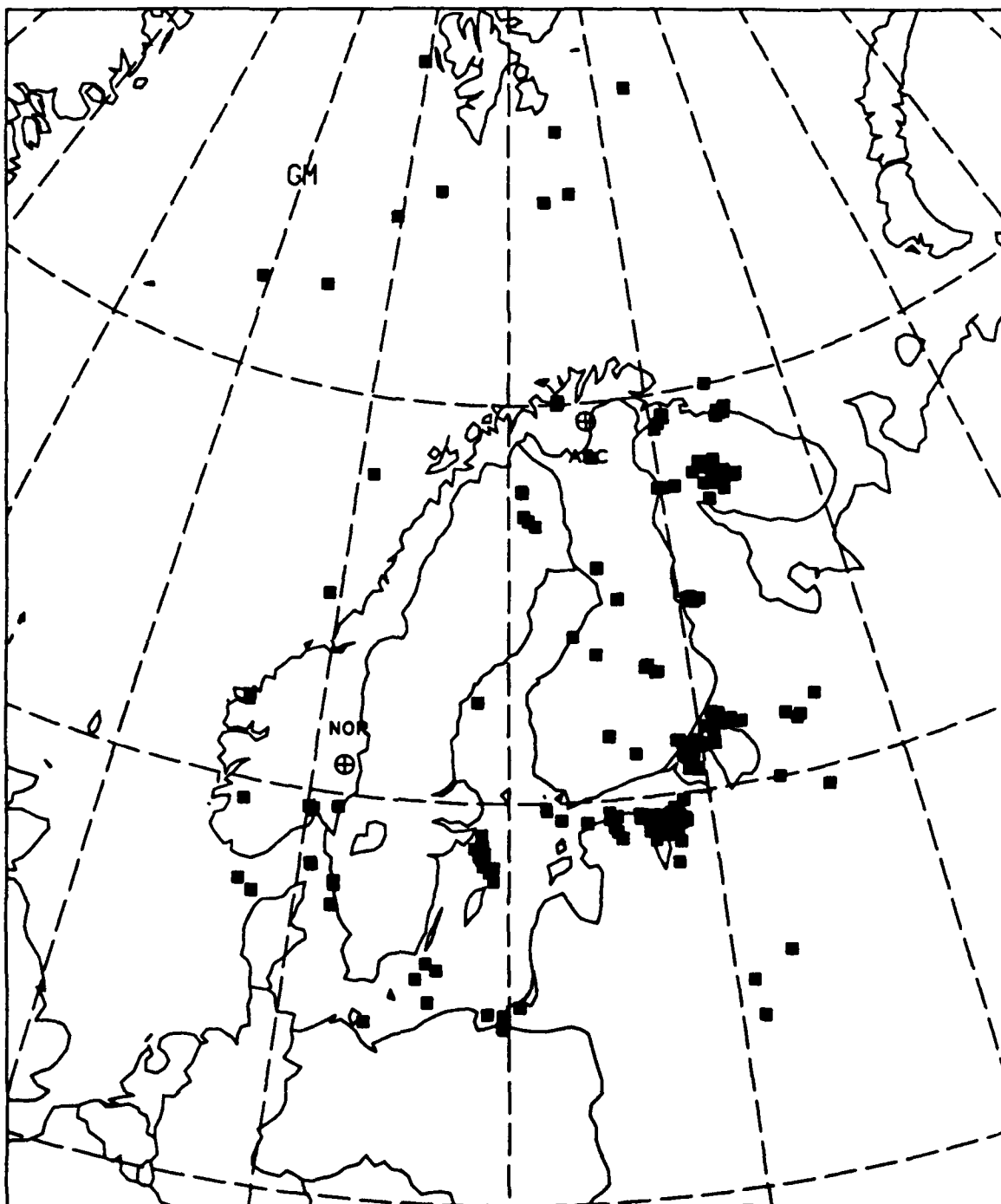


Figure 3. Epicenters are plotted for the 241 events with waveforms in Data Set #1.

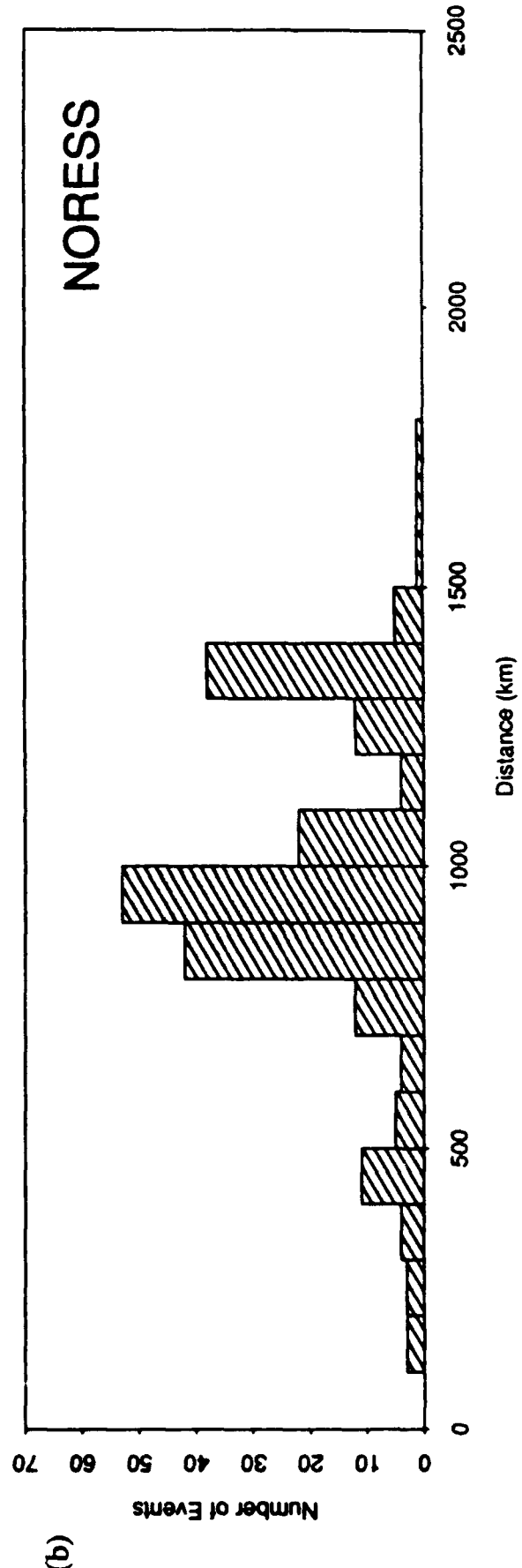
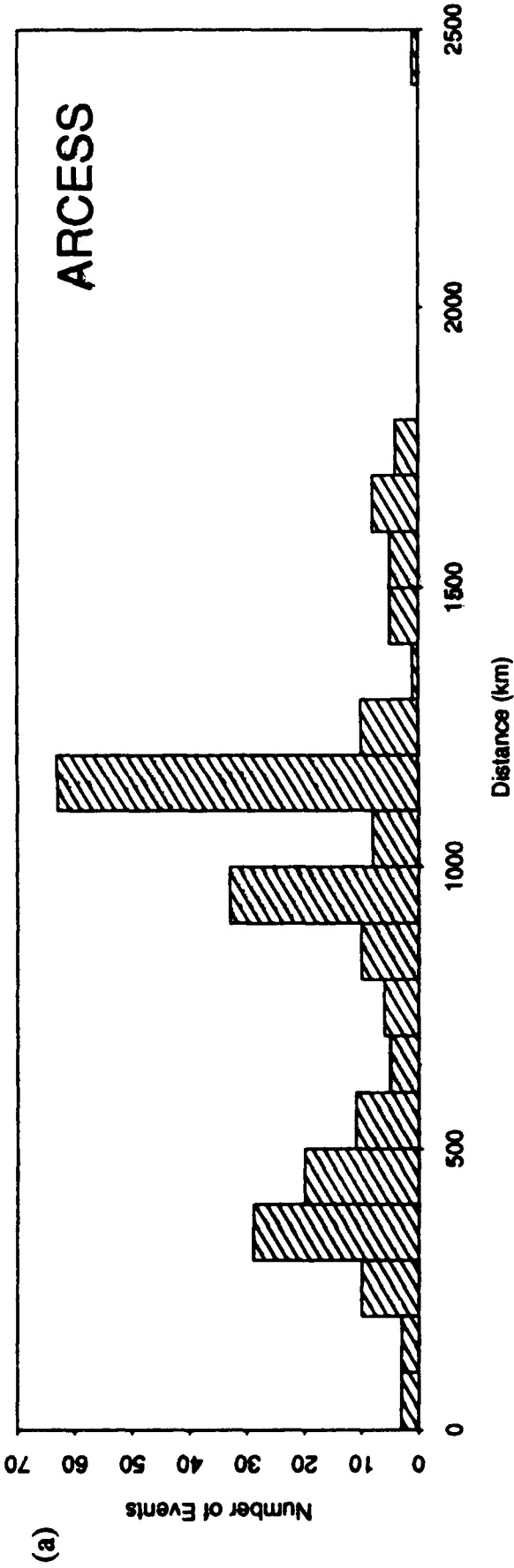


Figure 4. Histograms of epicentral distance to the events in Data Set #1 are plotted for (a) ARCESS, and (b) NORESS.

Magnitude Distribution - Data Set #1

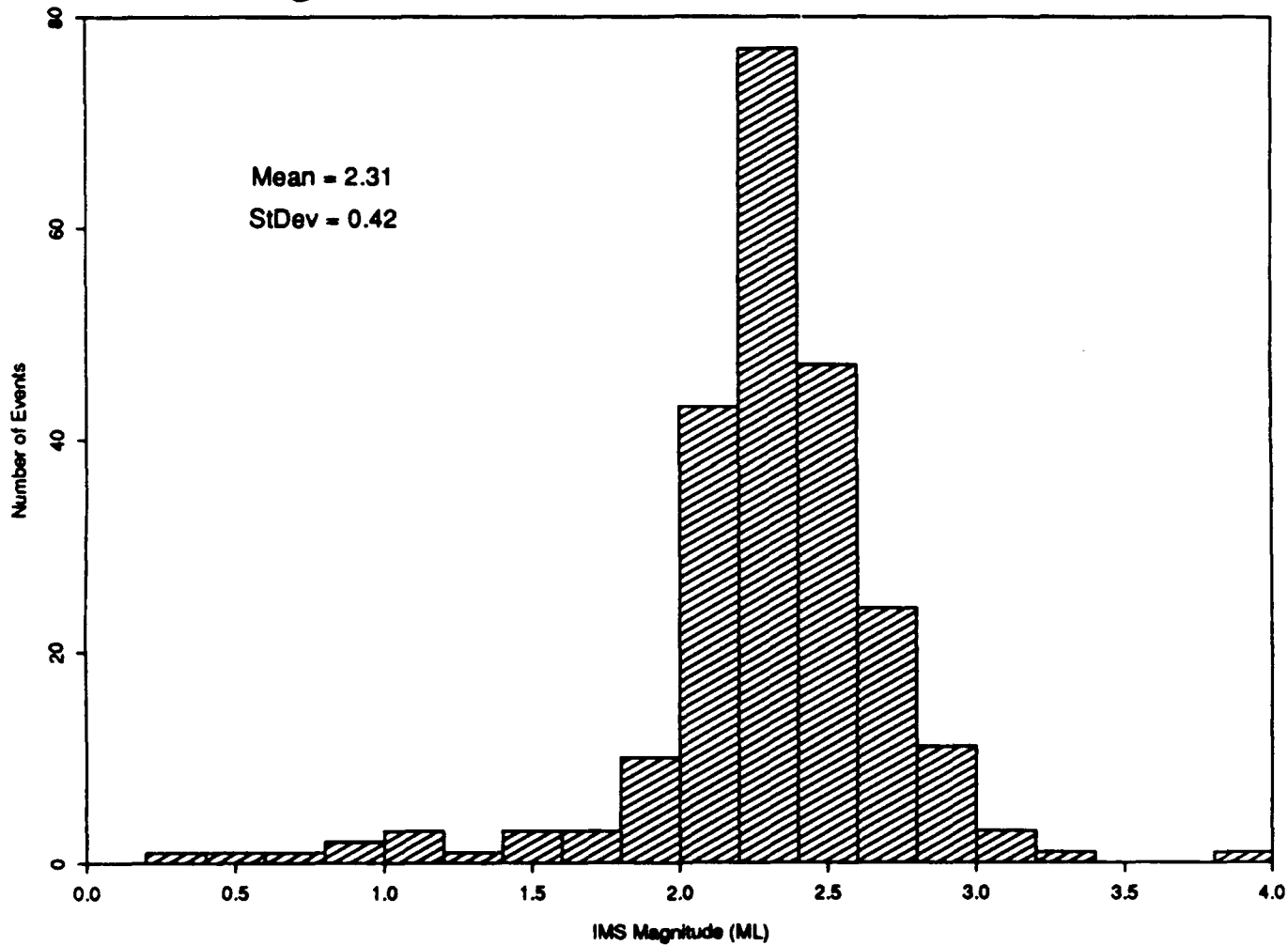
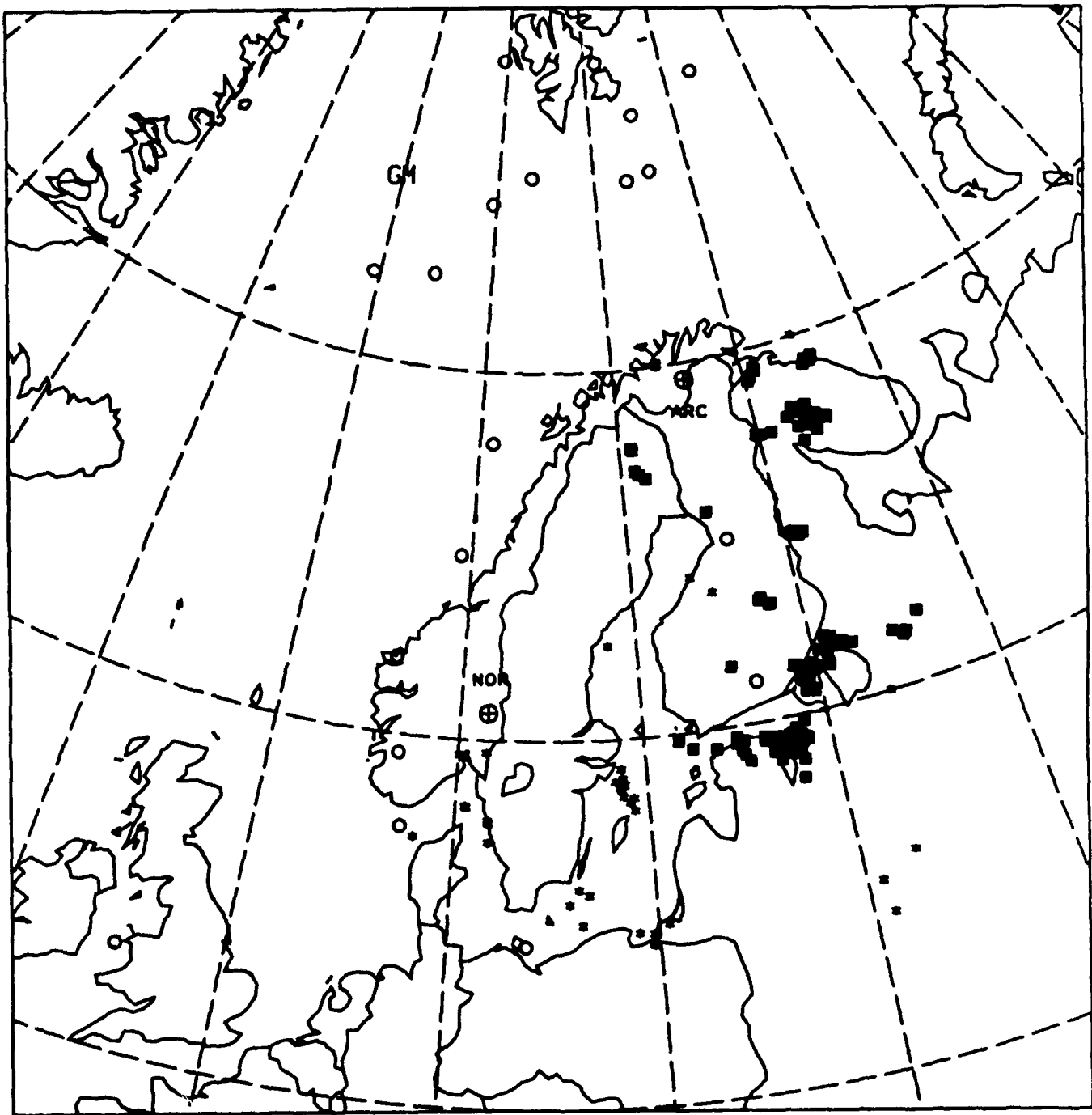


Figure 5. A histogram of L_g magnitude is shown for events in Data Set #1. The mean M_L is 2.31, and the standard deviation is 0.42.

Event Identification - Data Set #1



○ Earthquake ■ Mine Blast * Explosion

Figure 6. This map shows the locations of earthquakes (circles), mine blasts (squares), and other explosions (asterisks) in Data Set #1.

Events With Only Parametric Data (DB9) - Data Set #1

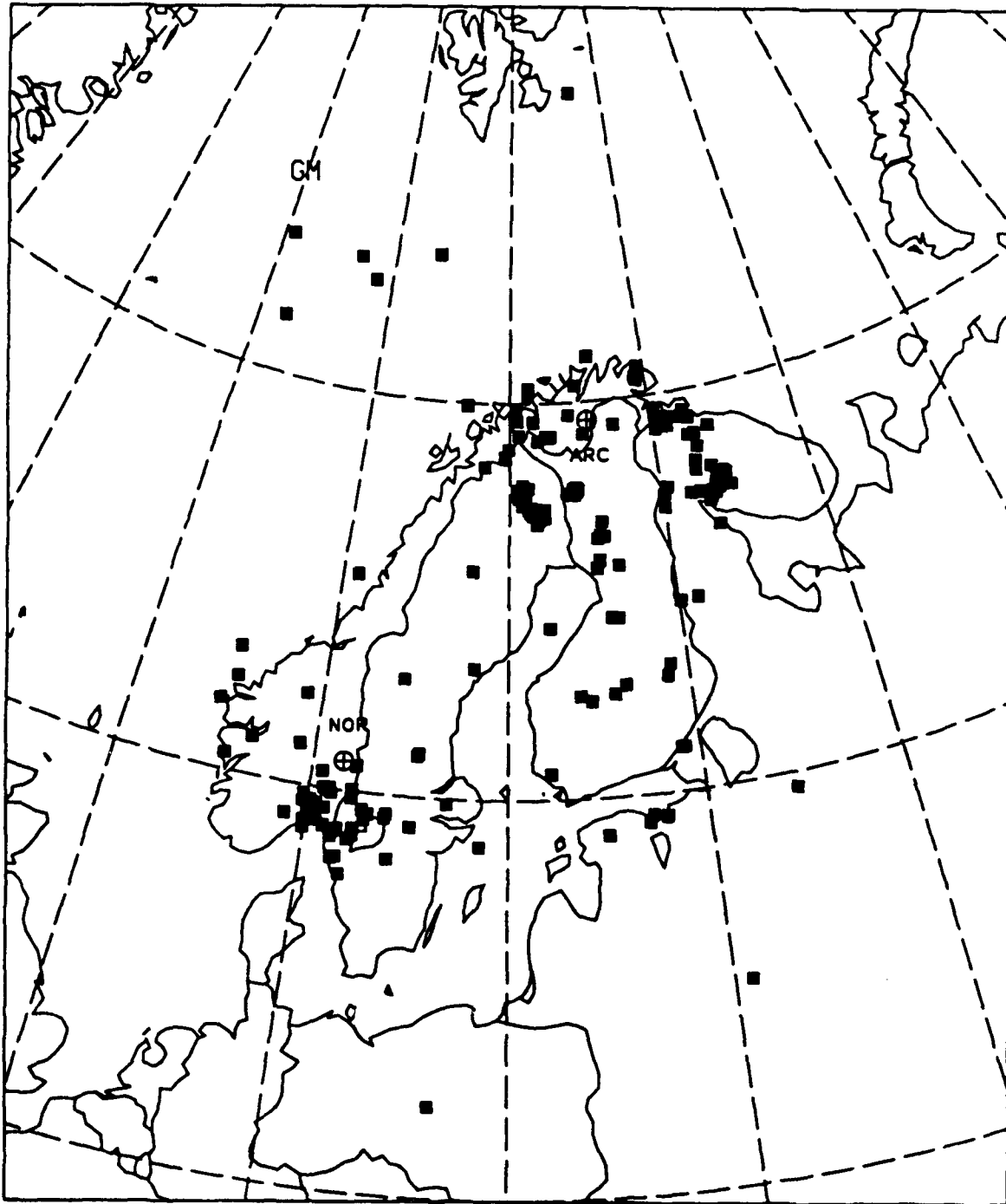


Figure 7. Epicenters are plotted for the 249 events with only parametric data (DB9) in Data Set #1.

2.3 Data Exchange Format

This section describes the exchange format for Data Set #1. These data were provided to *MIT* Lincoln Laboratory on read/write optical disks, but they are also available on 9-track tapes in UNIX tar format. Database reports that include hard-copy displays and information for each event were also provided to *MIT* Lincoln Laboratory. For each event, these reports include a map showing station and event location, a listing of event origin and detection data, the standard waveform display that is provided to the *IAS* seismic analyst, and plots of each detecting and 3-component beam (described below). Separate reports were provided for DB1, DB2, DB3, DB8, DB9, DB10, and DB11 [*Patnaik and Sereno, 1990a*].

Data Set #1 includes parametric data generated by the automated *IAS* processing, and all changes made by seismic analysts. It also includes all available short-period waveform data recorded at NORESS and ARCESS when the same event is detected by both arrays. The parametric data are stored as ASCII files, and the waveform data are stored in the binary format used by *SAC* (*Seismic Analysis Code*). *SAC* is a widely-used interactive analysis software package that was developed by Joseph Tull at Lawrence Livermore National Laboratory. Section 2.3.1 briefly describes the parametric data. The formats of the ASCII data files are described in detail in Appendix A. The waveform data are described in Section 2.3.2. An example of the displays and data that are included in each database report is given in Section 2.3.3.

2.3.1 Parametric Data

Figure 8 shows the directory structure for Data Set #1 (directories are printed in bold-face type, and files are printed in italics). The top-level directory includes sub-directories for each of the databases listed in Table 3, and sub-directories for documentation and static data (e.g., data that are the same for all events). The documentation directory includes a description of the data exchange format, and a description of several minor enhancements that we made to *SAC*. The static data include beam recipe files (described below), the NORESS/ARCESS short-period instrument response, the travel-time tables for regional phases used in *IAS*, and the locations of the individual stations in each array.

The general directory structure for each database is shown in the middle of Figure 8. Each database directory includes up to four sub-directories, and two ASCII files. The *README* file gives information for a few specific events. The *ExpSys_Analyst.dbX* file summarizes corrections made by the analyst to the results of the automated processing (the variable *X* appended to a file name or directory stands for the database number). For example, it includes the distance between the locations determined by the expert system and the analyst, the difference in their origin times, and the number of phases that were added or retimed by the analyst (see Appendix A).

The *ExpSys* directory contains the results of the automated *IAS* processing. This includes the four files in Figure 8 with the prefix *IEB*, which stands for initial event bulletin. *IEB.orig* lists event origin data (latitude, longitude, depth, and origin time). *IEB.det* lists detection and association data such as phase identification, arrival time,

DIRECTORY STRUCTURE / DATA SET #1

Top-Level Directory

DB1 DB2 DB3 DB8 DB9 DB10 DB11 doc static

Database Directory

DBX

README	ExpSys	Analyst	EVID	SAC
ExpSys_Analyst.dbX	IEB.orig	FEB.orig	README	oridXXXXX
	IEB.det	FEB.det	EVID.dbX	oridXXXXX
	IEB.apma	FEB.distaz	Helsinki orig	oridXXXXX
	IEB.sbsnr		Helsinki bul.dbX	etc
			MSMP.dbX	
			CEPPKS.dbX	
			SPVAR.dbX	

SAC Waveform Directory

SAC/oridXXXXX

ARA0.se.sac	ARC4.se.sac	ARD9.sz.sac	NRC3.sz.sac	NRD8.sz.sac
ARA0.sn.sac	ARC4.sn.sac	NRA0.se.sac	NRC4.se.sac	NRD9.sz.sac
ARA0.sz.sac	ARC4.sz.sac	NRA0.sn.sac	NRC4.sn.sac	ARC.cbxxx.sac
ARA1.sz.sac	ARC5.sz.sac	NRA0.sz.sac	NRC4.sz.sac	ARC.cbxxx.sac
ARA2.sz.sac	ARC6.sz.sac	NRA1.sz.sac	NRC5.sz.sac	ARC.cbxxx.sac
ARA3.sz.sac	ARC7.se.sac	NRA2.sz.sac	NRC6.sz.sac	ARC.cbxxx.sac
ARB1.sz.sac	ARC7.sn.sac	NRA3.sz.sac	NRC7.se.sac	ARC.cbxxx.sac
ARB2.sz.sac	ARC7.sz.sac	NRB1.sz.sac	NRC7.sn.sac	ARC.cbxxx.sac
ARB3.sz.sac	ARD1.sz.sac	NRB2.sz.sac	NRC7.sz.sac	ARC.cbxxx.sac
ARB4.sz.sac	ARD2.sz.sac	NRB3.sz.sac	NRD1.sz.sac	NOR.cbxxx.sac
ARB5.sz.sac	ARD3.sz.sac	NRB4.sz.sac	NRD2.sz.sac	NOR.cbxxx.sac
ARC1.sz.sac	ARD4.sz.sac	NRB5.sz.sac	NRD3.sz.sac	NOR.cbxxx.sac
ARC2.se.sac	ARD5.sz.sac	NRC1.sz.sac	NRD4.sz.sac	NOR.cbxxx.sac
ARC2.sn.sac	ARD6.sz.sac	NRC2.se.sac	NRD5.sz.sac	NOR.cbxxx.sac
ARC2.sz.sac	ARD7.sz.sac	NRC2.sn.sac	NRD6.sz.sac	
ARC3.sz.sac	ARD8.sz.sac	NRC2.sz.sac	NRD7.sz.sac	

Figure 8. The directory structure is described for Data Set #1.

azimuth and phase velocity estimated from $f-k$ processing, amplitude, signal-to-noise ratio, and frequency. *IEB.apma* lists results from automated particle motion analysis [Jurkevics, 1988]. This includes estimates of rectilinearity, planarity, long- and short-axis incidence angles, and horizontal-to-vertical power ratio for each detection. *IEB.sbsnr* gives signal and noise amplitudes measured on a standard set of six beams.

The **Analyst** directory contains parametric data after review by a seismic analyst. The files *FEB.orig* and *FEB.det* are similar to the corresponding files under **ExpSys**, but they include changes made by the analyst (the *FEB* prefix stands for final event bulletin). *FEB.distaz* lists the epicentral distance and station-to-event azimuth from NORESS and ARCESS for each event in *FEB.orig*. The **Analyst** directory does not include particle motion or standard-beam amplitude files since these attributes are not recalculated after analyst review.

The **EVID** directory contains the identification (e.g., earthquake or explosion) of each event in *FEB.orig*. This identification is based primarily on a regional seismic bulletin produced by the University of Helsinki. The *README* file gives information for a few specific events. *EVID.dbX* gives the identification of each event, *Helsinki.orig* gives the origin information from the Helsinki Bulletin, and *Helsinki.bul.dbX* gives the complete unedited listing from Helsinki Bulletin. The other three files in this directory contain data that are relevant for event identification. *MSMP.dbX* lists regional P -wave magnitudes computed from the amplitude of P_n and P_g , and regional S -wave magnitudes computed from the amplitude of S_n and L_g . The difference between these magnitudes is a possible discriminant (high values of $m_s - m_p$ indicate the event is an earthquake, low values are inconclusive). The two files called *CEPPKS.dbX* and *SPVAR.dbX* give the results of cepstral analysis, and are useful for identifying ripple-fired mining explosions [Baumgardt and Ziegler, 1987]. These data are described in Appendix A.

2.3.2 Waveform Data

The **SAC** sub-directory contains the NORESS and ARCESS waveform data in SAC format. There is a separate directory for each event. These directories are labeled as *oridXXXXXX*, where *XXXXXX* refers to the unique integer origin identification in *FEB.orig*. There are separate SAC data files for each short-period channel in the NORESS and ARCESS arrays (33 channels/array). These waveform data files are 7-minute segments that start 30 seconds before the theoretical P_n arrival time (based on the final event origin). The files are named as *station.channel.sac* where *station* is the station code for each array element (e.g., *NRA0*, *NRA1*, *NRA2*, etc), and *channel* is the channel code (*sz* is short-period vertical, *se* is short-period east, and *sn* is short-period north).

In addition to the single-channel waveforms, each directory includes several coherent beams in SAC format. Coherent beams are formed by steering the single-channel waveforms using a specified velocity and azimuth, stacking, and filtering over a specified frequency band. These files are named as *array.cbxxx.sac*, where *array* is either *NCR* for NORESS or *ARC* for ARCESS, *cb* stands for coherent beam, and *xxx* is the beam number in the first column of Table 6 (this table describes the beam set

Table 6. IAS Beam Deployment

Beam	Velocity (km/s)	Filter (Hz)	Filter Order	Azimuth (degrees)	Beam Type ¹	Ring Subset			
201	∞	1.0-3.0	3	0.0	C	A0		C	D
202	∞	1.5-3.5	3	0.0	C	A0		C	D
207	∞	8.0-16.0	3	0.0	C	A0	A	B	
220	∞	1.5-2.5	2	0.0	I	A0		C	
221	∞	2.0-4.0	3	0.0	H	A0		C	
223	∞	5.0-10.0	3	0.0	H	A0		C	
225	∞	3.5-5.5	3	0.0	I	A0		C	
226	∞	3.5-5.5	3	0.0	H	A0		C	
228	∞	8.0-16.0	3	0.0	H	A0		C	
248	11.0	1.5-3.5	3	30.0	C	A0		C	D
249	11.0	1.5-3.5	3	90.0	C	A0		C	D
250	11.0	1.5-3.5	3	150.0	C	A0		C	D
251	11.0	1.5-3.5	3	210.0	C	A0		C	D
252	11.0	1.5-3.5	3	270.0	C	A0		C	D
253	11.0	1.5-3.5	3	330.0	C	A0		C	D
254	∞	2.0-4.0	3	0.0	C	A0		C	D
255	10.1	2.0-4.0	3	30.0	C	A0		C	D
256	10.1	2.0-4.0	3	90.0	C	A0		C	D
257	10.1	2.0-4.0	3	150.0	C	A0		C	D
258	10.1	2.0-4.0	3	210.0	C	A0		C	D
259	10.1	2.0-4.0	3	270.0	C	A0		C	D
260	10.1	2.0-4.0	3	330.0	C	A0		C	D
261	∞	2.5-4.5	3	0.0	C	A0	B	C	
262	8.8	2.5-4.5	3	30.0	C	A0	B	C	D
263	8.8	2.5-4.5	3	90.0	C	A0	B	C	D
264	8.8	2.5-4.5	3	150.0	C	A0	B	C	D
265	8.8	2.5-4.5	3	210.0	C	A0	B	C	D
266	8.8	2.5-4.5	3	270.0	C	A0	B	C	D
267	8.8	2.5-4.5	3	330.0	C	A0	B	C	D
268	∞	3.0-5.0	3	0.0	C	A0	B	C	D
269	10.5	3.0-5.0	3	30.0	C	A0	B	C	D
270	10.5	3.0-5.0	3	90.0	C	A0	B	C	D
271	10.5	3.0-5.0	3	150.0	C	A0	B	C	D
272	10.5	3.0-5.0	3	210.0	C	A0	B	C	D
273	10.5	3.0-5.0	3	270.0	C	A0	B	C	D
274	10.5	3.0-5.0	3	330.0	C	A0	B	C	D
275	∞	3.5-5.5	3	0.0	C	A0	B	C	
276	11.1	3.5-5.5	3	30.0	C	A0	B	C	
277	11.1	3.5-5.5	3	90.0	C	A0	B	C	
278	11.1	3.5-5.5	3	150.0	C	A0	B	C	
279	11.1	3.5-5.5	3	210.0	C	A0	B	C	
280	11.1	3.5-5.5	3	270.0	C	A0	B	C	
281	11.1	3.5-5.5	3	330.0	C	A0	B	C	
282	∞	4.0-8.0	3	0.0	C	A0	B	C	
283	9.4	4.0-8.0	3	30.0	C	A0	B	C	
284	9.4	4.0-8.0	3	90.0	C	A0	B	C	
285	9.4	4.0-8.0	3	150.0	C	A0	B	C	
286	9.4	4.0-8.0	3	210.0	C	A0	B	C	
287	9.4	4.0-8.0	3	270.0	C	A0	B	C	
288	9.4	4.0-8.0	3	330.0	C	A0	B	C	

Beam	Velocity (km/s)	Filter (Hz)	Filter Order	Azimuth (degrees)	Beam Type ¹	Ring Subset				
289	∞	5.0-10.0	3	0.0	C	A0		B	C	
290	10.4	5.0-10.0	3	30.0	C	A0		B	C	
291	10.4	5.0-10.0	3	90.0	C	A0		B	C	
292	10.4	5.0-10.0	3	150.0	C	A0		B	C	
293	10.4	5.0-10.0	3	210.0	C	A0		B	C	
294	10.4	5.0-10.0	3	270.0	C	A0		B	C	
295	10.4	5.0-10.0	3	330.0	C	A0		B	C	
296	9.9	8.0-16.0	3	30.0	C	A0	A	B		
297	9.9	8.0-16.0	3	90.0	C	A0	A	B		
298	9.9	8.0-16.0	3	150.0	C	A0	A	B		
299	9.9	8.0-16.0	3	210.0	C	A0	A	B		
300	9.9	8.0-16.0	3	270.0	C	A0	A	B		
301	9.9	8.0-16.0	3	330.0	C	A0	A	B		
302	15.9	1.5-3.5	3	80.0	C	A0			C	D
303	15.9	2.0-4.0	3	80.0	C	A0			C	D
304	15.9	2.5-4.5	3	80.0	C	A0		B	C	D
305	15.9	3.0-5.0	3	80.0	C	A0		B	C	D
306	10.0	1.5-3.5	3	30.0	C	A0			C	D
307	10.0	2.0-4.0	3	30.0	C	A0			C	D
308	10.0	2.5-4.5	3	30.0	C	A0		B	C	D
309	10.0	3.0-5.0	3	30.0	C	A0		B	C	D
310	∞	1.0-2.0	2	0.0	I	A0			C	
312	∞	2.0-4.0	3	0.0	I	A0			C	
313	∞	2.0-3.0	2	0.0	I	A0			C	

1. C = Coherent, I = Incoherent (vertical channels), H = Incoherent (horizontal channels)

applied to NORESS and ARCESS during the operation of IAS). The *detecting beam* is defined as the standard beam in Table 6 with the highest *snr*. This beam is included for each detection that is associated with a final origin. However, if the *detecting beam* is incoherent, then it is replaced by a coherent beam that uses the same beam-forming parameters.

Coherent beams that are calculated using data from the four 3-component elements of each array are also included in Data Set #1. Three of these beams are calculated for each detection that is associated with a final event origin (one for each component; vertical, north-south, and east-west). These 3-component beams use the same beamforming parameters as the *detecting beam*, except that the array subset only includes the four 3-component elements. The number assigned to the beam formed from the vertical components is 200 plus the beam number of the *detecting beam*. Similarly, the numbers assigned to the beams formed from the north-south and east-west components are 400 and 600 plus the beam number of the *detecting beam*, respectively.

2.3.3 Database Reports

This section gives an example of the displays and information that are included in the database reports provided to MIT Lincoln Laboratory [Patnaik and Sereno, 1991a]. This example is for a mining explosion in western USSR. Figure 9 is a map showing the locations of NORESS and ARCESS, and the event epicenter. Table 7 lists detection data before analyst review (e.g., the results of the automated IAS processing), and Table 8 lists detection data after analyst review. Figure 10 shows the *display beams* for ARCESS (this is the standard waveform display that is provided to the IAS seismic analyst). Figure 11 plots the *detecting beam* for P_n at ARCESS, and the 3-component beams (vertical, north-south, and east-west). Similarly, Figure 12 plots the beams for S_n at ARCESS. Beams are not included for L_g since this phase was added by the analyst (e.g., it was not detected by the automated processing). Figure 13 shows the *display beams* for NORESS, and Figure 14 shows the *detecting* and 3-component beams for P_n at NORESS. Beams were not computed for S_n and L_g phases at NORESS because they were added by the analyst.

ORID=192093 90/02/14 10 16 5.013 LAT 61.70 LON 31.37 ML 2.2

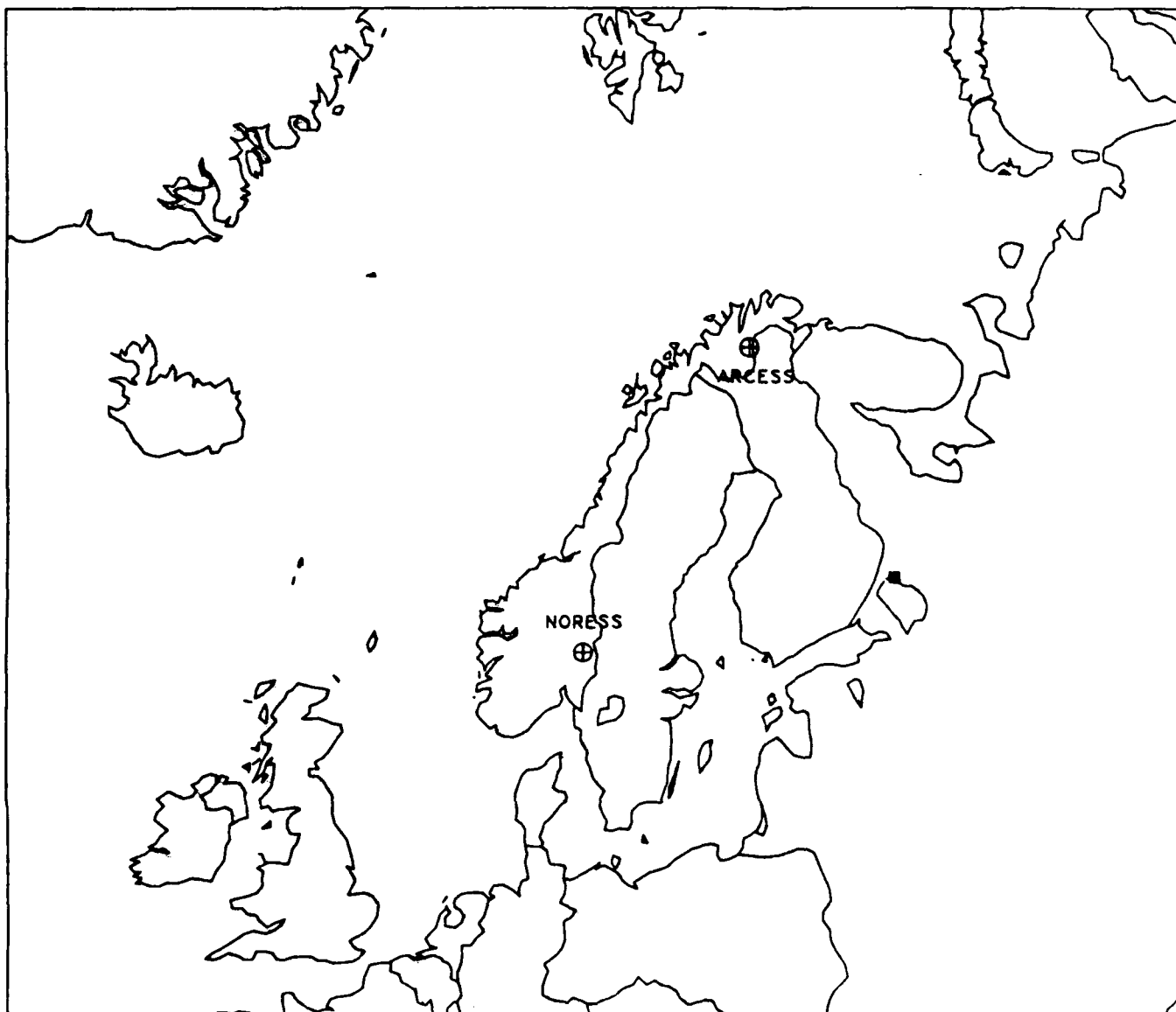


Figure 9. This map shows the NORESS and ARCESS station locations, and the epicenter of an event in Data Set #1 (after analyst review).

BOIID	ARID STA	CHAN	CHANID	YR	MM	DD	HR:MM:SS.MS	IPHASE	PHASE	AMP	FREQ	SNR	VELO	AZIMUTH Q
195318	129358 ARAO	zb	292	90	02	14	10:18:05.332	Pg	Pg	163.9	6.7	8.58	7.7	154.9 1
-1	129359 ARAO	zb	272	90	02	14	10:18:09.582	Px	-----	61.5	3.3	4.23	7.5	165.11 3
195318	129363 ARAO	zb	275	90	02	14	10:18:24.384	Pg	Pg	155.8	4.3	10.76	10.9	87.06 1
195319	129360 ARAO	zb	294	90	02	14	10:19:33.982	Lg	Lg	107.5	6.7	4.74	4.6	164.96 2
-1	129364 ARAO	zb	296	90	02	14	10:19:35.859	Sx	-----	99.5	10.0	5.24	3.7	251.01 3
-1	129365 ARAO	zb	310	90	02	14	10:20:13.857	Px	-----	954.5	1.2	2.55	6.3	34.05 3
-1	129366 ARAO	zb	301	90	02	14	10:22:01.632	Sx	-----	49.2	6.7	4.88	3.2	181.13 3
-1	129367 ARAO	zb	225	90	02	14	10:23:08.107	Sx	-----	131.0	4.5	2.46	3.0	176.52 1

Table 7. This table gives parametric detection and phase association data before analyst review for the event plotted in Figure 9. Two phases were associated with this event by the expert system (arid 129358 is labeled Pg at ARCESS, and arid 129363 is labeled Pg at NORESS).

FORID	ARID STA	CHAN	CHANID	YR	MM	DD	HR	MM	SS	MS	IPHASE	PHASE	AMP	FREQ	SNR	VELO	AZIMUTH	Q
192093	129358 ARAO	zb	292	90	02	14	10:16:02	.514	Pn		Pn	163.9	6.7	8.58	7.7	154.9	1	
-1	129359 ARAO	zb	272	90	02	14	10:16:09	.582	Px			61.5	3.3	4.23	7.5	165.11	3	
192093	129363 NRAO	zb	275	90	02	14	10:18:23	.871	Pn		Pn	155.8	4.3	10.76	10.9	87.06	1	
192093	129360 ARAO	zb	294	90	02	14	10:19:33	.982	Sn		Sn	107.5	6.7	4.74	4.6	164.96	2	
-1	129364 NRAO	zb	296	90	02	14	10:19:35	.859	Sx			99.5	10.0	5.24	3.7	251.01	3	
192093	130563 NRAO	-	-1	90	02	14	10:20:04	.312	Sn		Sn	-1.0	-1.0	-1	-1.0	-1	-	
-1	129365 ARAO	zb	310	90	02	14	10:20:13	.857	Px			954.5	1.2	2.55	6.3	34.05	3	
192093	130562 ARAO	-	-1	90	02	14	10:20:26	.051	Lg		Lg	-1.0	-1.0	-1	-1.0	-1	-	
192093	130564 NRAO	-	-1	90	02	14	10:21:05	.305	Lg		Lg	-1.0	-1.0	-1	-1.0	-1	-	
-1	129366 ARAO	zb	301	90	02	14	10:22:01	.632	Sx			49.2	6.7	4.88	3.2	181.13	3	
-1	129367 ARAO	zb	225	90	02	14	10:23:08	.107	Sx			131.0	4.5	2.46	3.0	176.52	1	

Table 8. This table gives parametric detection and phase association data after analyst review for the event plotted in Figure 9. The analyst made the following changes to the results of the expert system (see Table 7):

- (1) Rename *Pg* at ARCESS to *Pn*, and retime.
- (2) Rename *Lg* at ARCESS to *Sn*, and associate it with this event.
- (3) Add an *Lg* phase at ARCESS (signal processing is not recalled for phases that are added by analyst, so most of the detection fields are assigned N/A values).
- (4) Rename *Pg* at NORESS to *Pn*, and retime.
- (5) Add an *Sn* phase at NORESS.
- (6) Add an *Lg* phase at NORESS.

The location determined by the expert system is about 250 km from the by location determined by the analyst for this event.

ORID = 192093 ARCESS

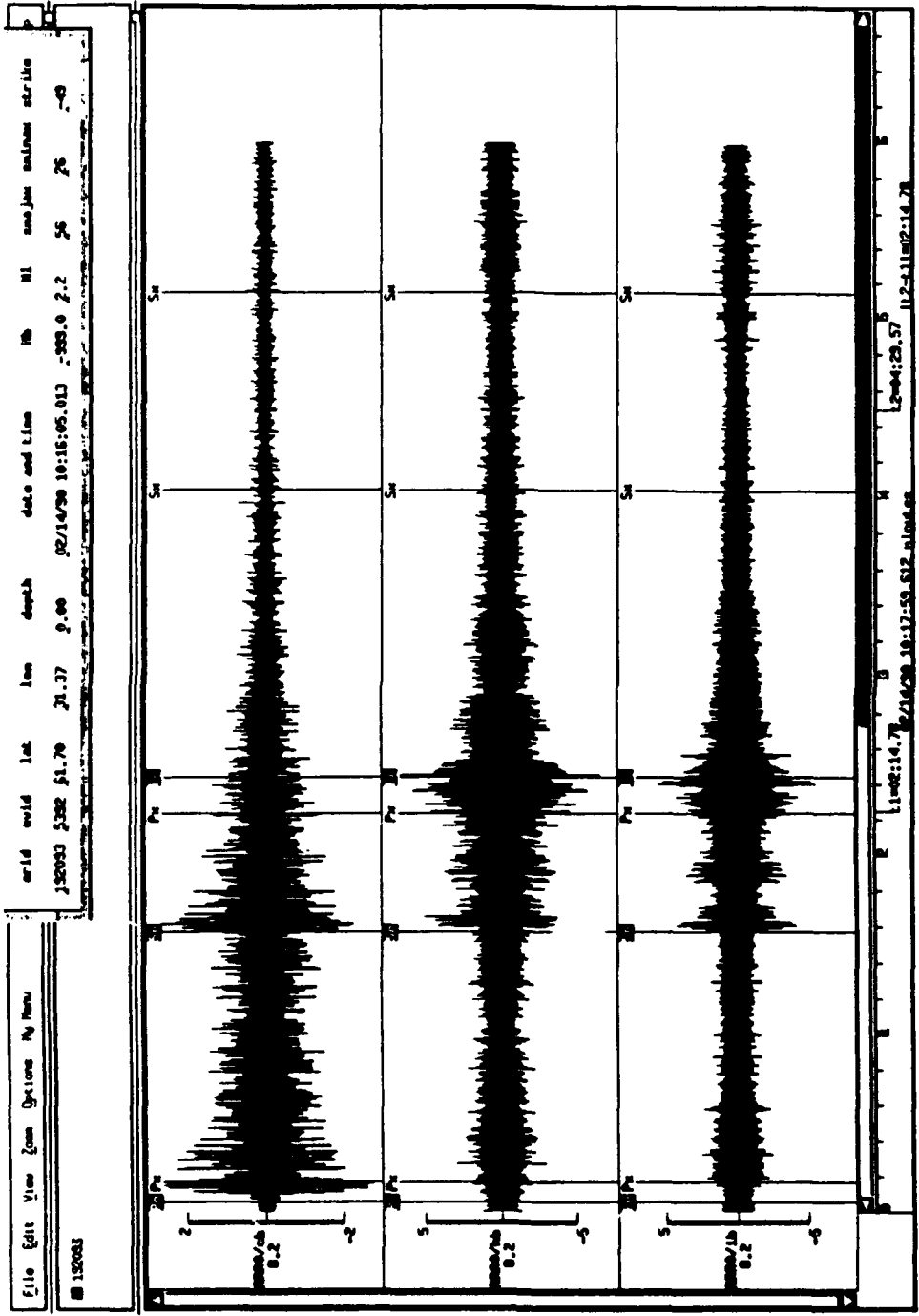


Figure 10. ARCESS display beams are plotted for the event in Figure 9. Associated Pn, Sn, and Lg phases are highlighted. The top beam is a 4-8 Hz coherent beam (steered to the event using a velocity of 8 km/s), and it is intended to emphasize Pn. The middle beam is a 2-4 Hz incoherent beam formed from horizontal components intended to emphasize Sn. The lowest beam is also a 2-4 Hz incoherent beam, but it is formed from vertical components. It is intended to emphasize Lg.

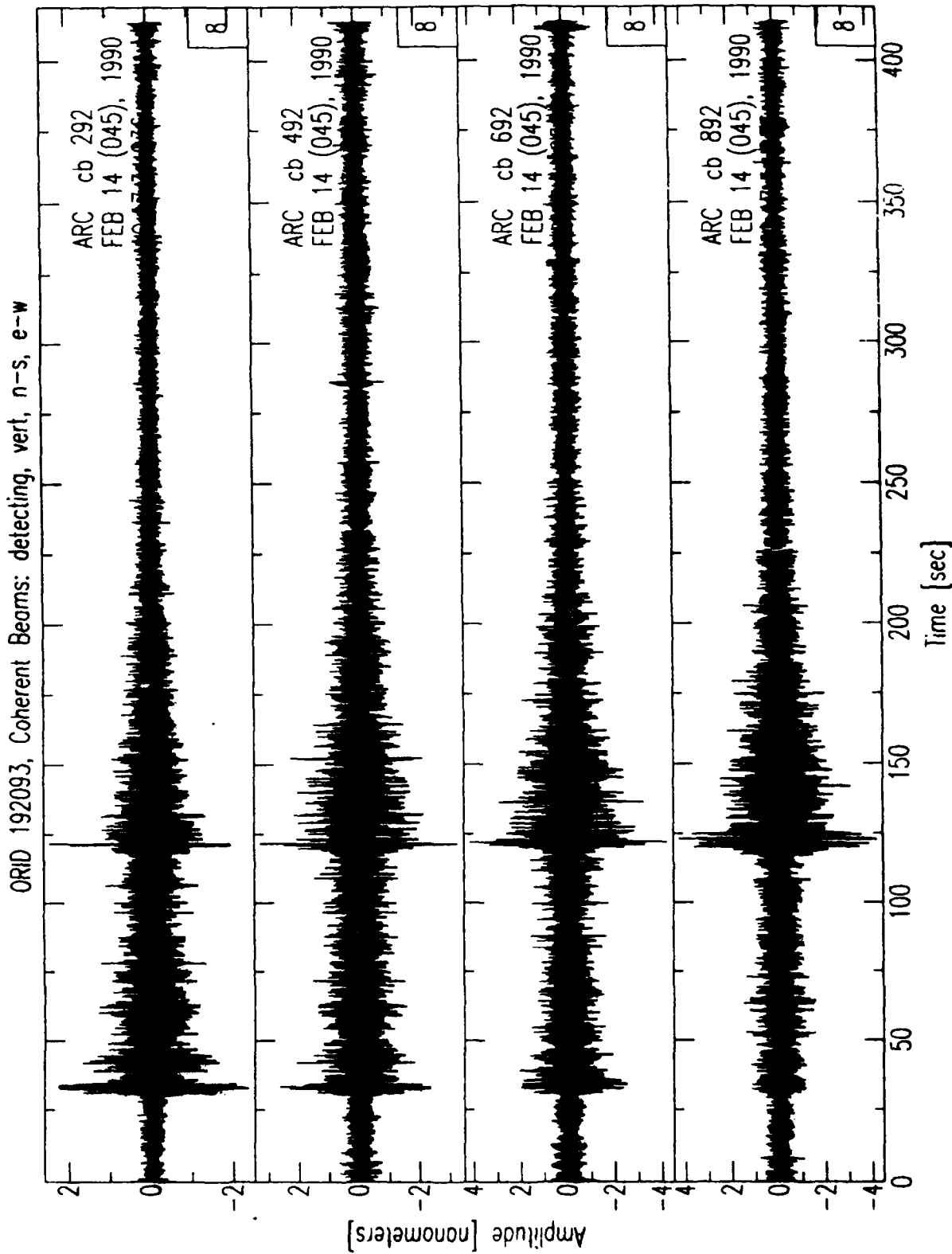


Figure 11. This figure shows the *detecting beam* for P_n at ARCESS in the top panel, and the beams formed from the 3-component array elements in the bottom panels (vertical, north-south, east-west).

ORID 192093, Coherent Beams: detecting, vert, n-s, e-w

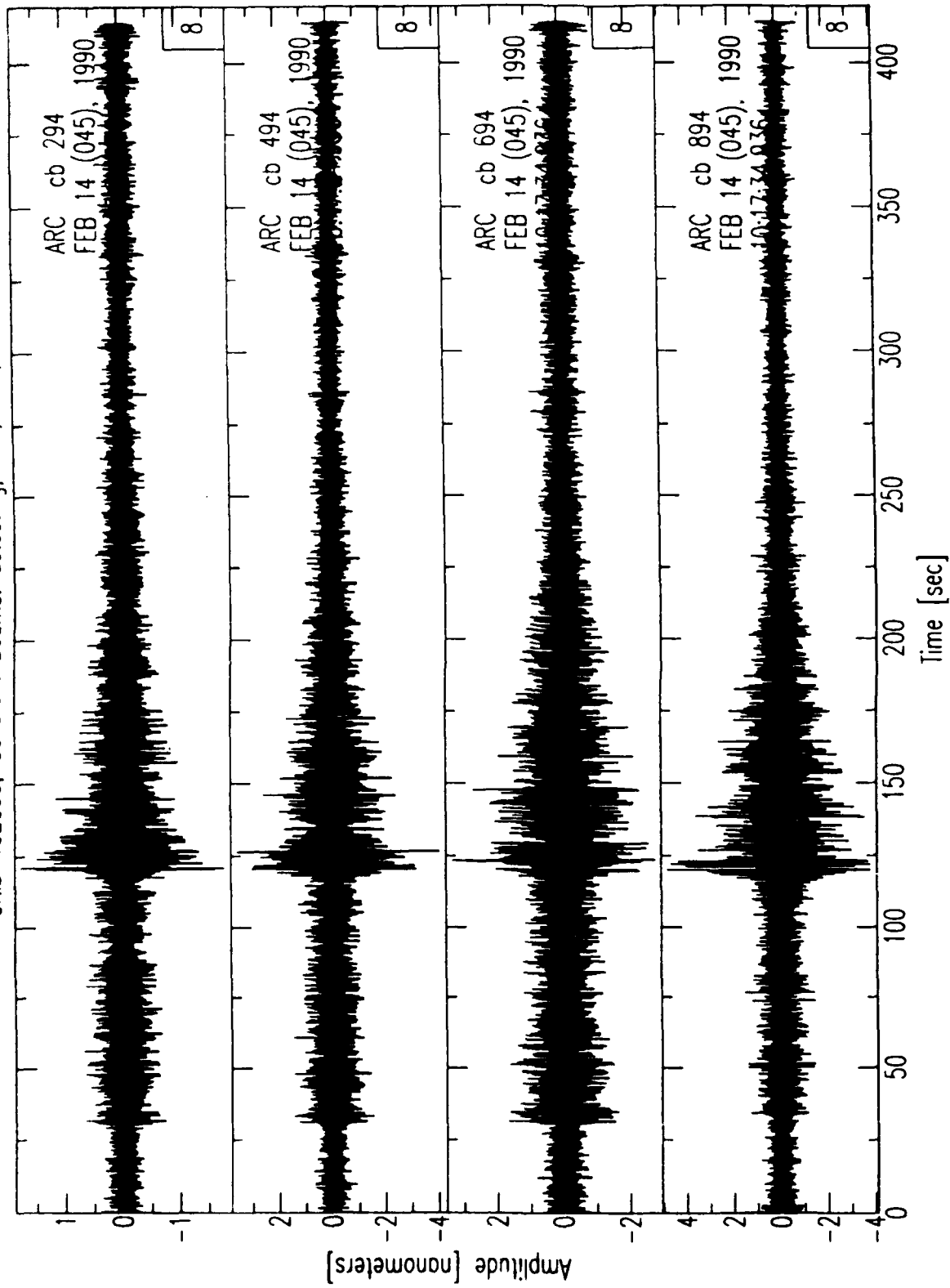


Figure 12. This figure shows the *detecting beam* for S_n at ARCESS in the top panel, and the beams formed from the 3-component array elements in the bottom panels (vertical, north-south, east-west).

ORID = 192093 NORESS

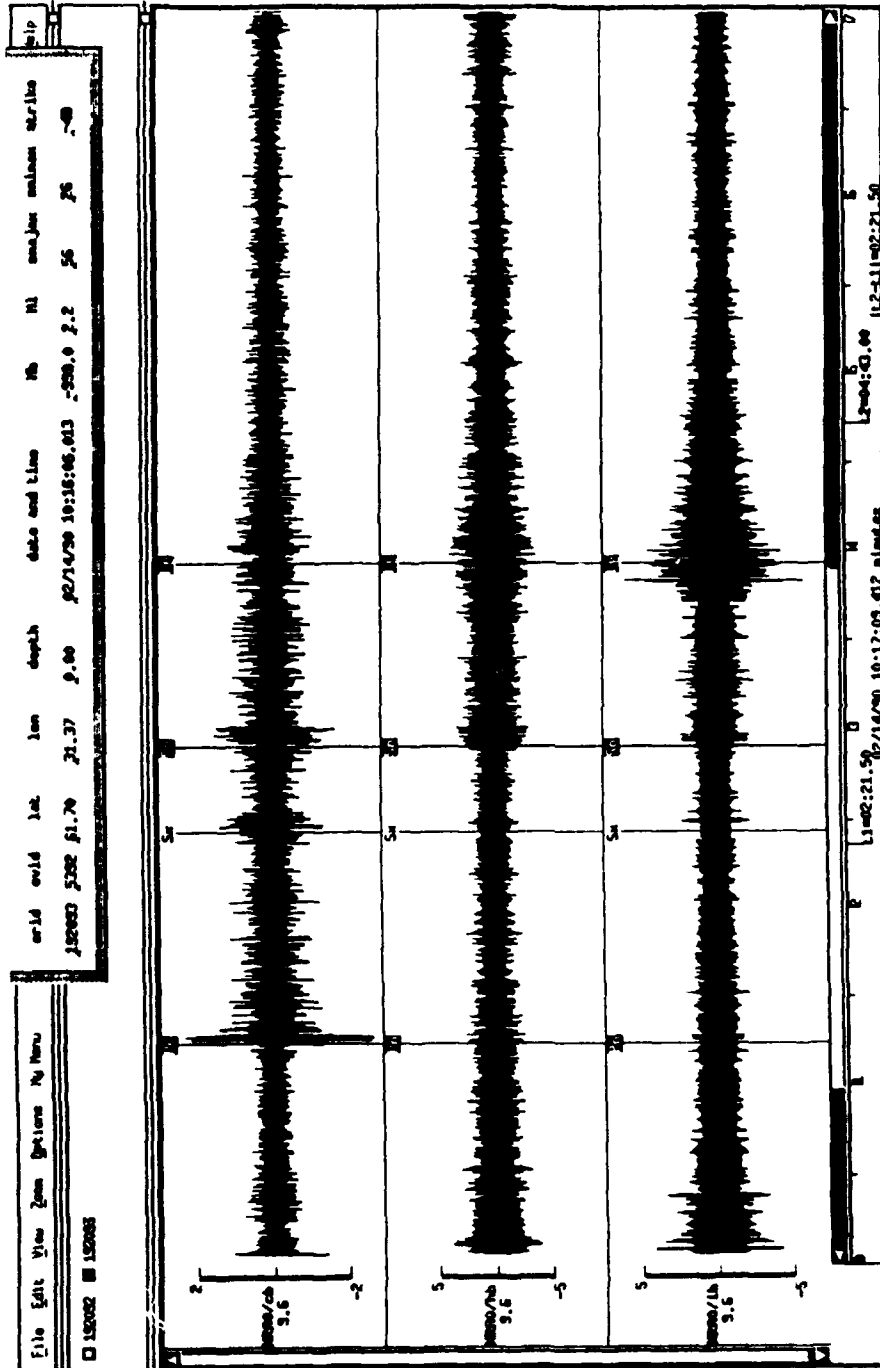


Figure 13. NORESS display beams are plotted for the event in Figure 9. Associated P_n , S_n , and L_g phases are highlighted (see caption for Figure 10).

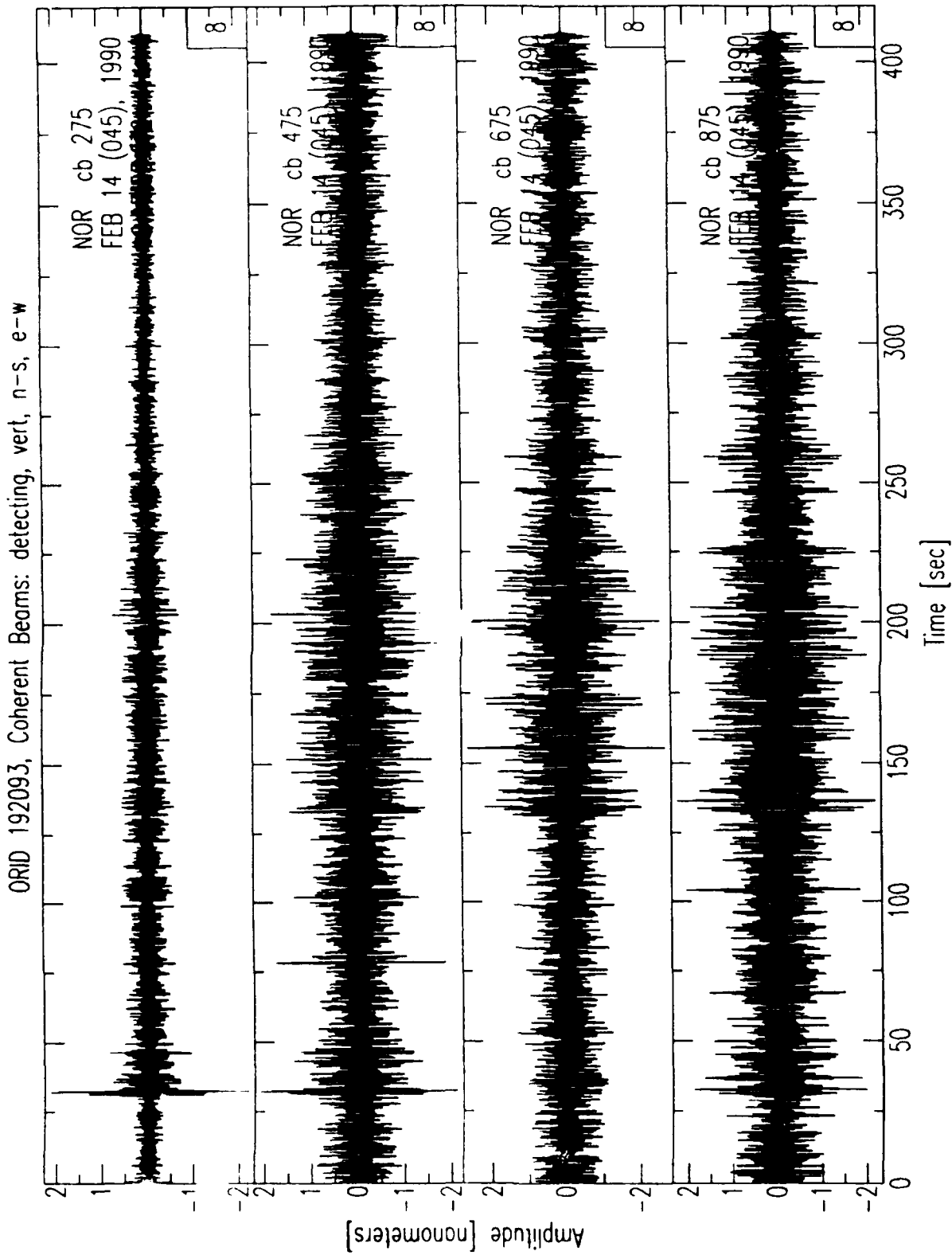


Figure 14. This figure shows the *detecting beam* for P_n at NORESS in the top panel, and the beams formed from the 3-component array elements in the bottom panels (vertical, north-south, east-west).

(THIS PAGE INTENTIONALLY LEFT BLANK)

3. SUMMARY

We developed a data set to test and evaluate the performance of neural networks for automated processing and interpretation of seismic data. This data set may also be valuable for many other studies related to seismic monitoring of nuclear explosion testing. It includes waveform and parametric data from 241 regional events recorded by the short-period elements of the NORESS and ARCESS arrays in Norway (33 channels/array). The waveform data are stored in SAC binary format, and the parametric data are stored in ASCII files. The event epicentral distances are 200-1800 km, and the event *Lg* magnitudes are approximately 1.5-3.2. Most of the events are mining explosions in western USSR, Sweden, and Finland. However, 18 of the events are earthquakes, and 22 are presumed underwater explosions. Detailed documentation has been developed for each event, and is included in eight separate database reports. The data and software are available at the Center for Seismic Studies.

ACKNOWLEDGMENTS

We thank Ann Suteau-Henson at the Center for Seismic Studies for sending us complete documentation on the automated particle motion analysis used in *IAS*. This research was funded by the Defense Advanced Research Projects Agency under Contract F19628-90-C-0156 and monitored by Phillips Laboratory.

(THIS PAGE INTENTIONALLY LEFT BLANK)

REFERENCES

- Anderson, J., W. Farrell, K. Garcia, J. Given, and H. Swanger, Center for Seismic Studies Version 3 Database: Schema Reference Manual, *Tech. Rep. C90-01*, Center for Seismic Studies, Arlington, VA., 1990.
- Bache, T., J. Anderson, D. Baumgardt, S. Bratt, W. Farrell, R. Fung, J. Given, A. Henson, C. Kobryn, H. Swanger, J. Wang, Intelligent Array System, *Final Tech. Rep. SAIC-90/1437*, Sci. Appl. Int. Corp., San Diego, Calif., 1990.
- Bache, T., S. Bratt, J. Given, T. Schroeder, H. Swanger, and J. Wang, The Intelligent Monitoring System Version 2, *Quarterly Tech. Rep. #6 SAIC-91/1137*, Sci. Appl. Int. Corp., San Diego, Calif., 1991.
- Baumgardt, D., and K. Ziegler, Spectral evidence for source multiplicity in explosions *Semiannu. Tech. Rep. SAS-TR-87-01*, Ensco, Inc., Springfield, VA, AFGL-TR-87-0045, ADA187363, 1987.
- Jurkevics, A., Polarization analysis of three-component array data, *Bull. Seismol. Soc. Am.*, 78, 1725-1743, 1988.
- LaCoss, R., R. Cunningham, S. Curtis, and M. Seibert, Artificial neural networks for seismic data interpretation, *Semiannu. Tech. Rep. ESD-TR-91-058*, Lincoln Laboratory, Massachusetts Institute of Technology, Lexington, MA, ADA239673, 1990.
- LaCoss, R., S. Curtis, R. Cunningham, and M. Seibert, Seismic phase and event labeling using artificial neural networks, Paper presented at the 13th Annual PL/DARPA Seismic Research Symposium, Keystone, CO, 8-10 October, 1991.
- Mykkeltveit, S., K. Astebol, D. Doornbos, and E. Husebye, Seismic array configuration optimization, *Bull. Seismol. Soc. Am.*, 73, 173-186, 1983.
- Mykkeltveit, S., and F. Ringdal, New results from processing of data recorded at the new ARCESS regional array, *Sci. Rep. 2-87/88*, NTNF/NORSAR, Kjeller, Norway, 1988.
- Patnaik, G., and T. Sereno, Data to test and evaluate the performance of neural network architectures for seismic signal discrimination - DARPA Data Set #1, *Tech. Rep. SAIC-91/1274 (Vol. 1-7)*, Sci. Appl. Int. Corp., San Diego, Calif., 1991a.
- Patnaik, G., and T. Sereno, Neural Computing For Seismic Phase Identification, *Annu. Tech. Rept. (Volume II) SAIC-91/1237*, Sci. Appl. Int. Corp., San Diego, Calif.,

1991b.

Sereno, T., Data to test and evaluate the performance of neural network architectures for seismic signal discrimination: Event identification - DARPA DataSet #1, *Tech. Rep. SAIC-91/1275*, Sci. Appl. Int. Corp., San Diego, Calif., 1991.

Swanger, H., J. Given, and J. Anderson, IMS extensions to the Center Version 3 Database, *Quarterly Tech. Rep. #5 SAIC-91/1138*, Sci. Appl. Int. Corp., San Diego, Calif., 1990.

Wahlström, R. and T. Ahjos, Magnitude determination of earthquakes in the Baltic Shield, *Annales Geophysicae*, 2, 553-558, 1984.

APPENDIX A: PARAMETRIC DATA EXCHANGE FORMAT

This appendix describes the parametric data files in Data Set #1 (Figure 2.8). These data were retrieved from the *IAS* relational database at the Center for Seismic Studies. Examples of each data file are given at the end of this section.

ExpSys_Analyst.dbX

Table A.1 *ExpSys_Analyst.dbX* Data File

ExpSys_Analyst.dbX			
attribute name	field no.	Storage type	attribute description
eorid	1	i4	expert system origin id
forid	2	i4	final origin id
ddist	3	f4	distance between forid and eorid
dtime	4	f4	origin time difference
rprimp	5	i4	no. of renamed primary phases
rsecondp	6	i4	no. of renamed secondary phases
added	7	i4	no. of added phases
retime	8	i4	no. of retimed phases

Table A.1 describes the *ExpSys_Analyst.dbX* data file. This file summarizes the corrections made by an analyst to the results of the automated processing. All of the attributes in this table were extracted from the *ex_an* database table at *CSS* which is an *IMS* extension to the Center Version 3 Database [Swanger *et al.*, 1991]. This file joins the *ExpSys* data files and the *Analyst* data files through the unique integer origin identifications, *eorid* and *forid*. The attributes have the following definitions:

- eorid*: A unique positive integer which identifies an origin determined by the expert system.
- forid*: A unique positive integer which identifies an origin determined (or validated) by a seismic analyst.
- ddist*: The distance between the event location determined by the expert system and the event location determined by the analyst (in kilometers).
- dtime*: The absolute value of the difference between the origin time estimated by the expert system and the origin time estimated by the analyst (in seconds).
- rprimp*: Number of primary (*P*-type) phases that were renamed by an analyst.
- rsecondp*: Number of secondary (*S*-type) phases that were renamed by an analyst.
- added*: Number of phases that were added by an analyst. These are phases that were not detected by the automated system.
- retime*: Number of phases that were retimed by an analyst.

There are cases in which fields 5–8 are zero, but the analyst and expert system solutions differ. This can happen if the analyst associates or disassociates a phase with the current event (the phase is not renamed, retimed, or added).

ExpSys

The ExpSys directory contains parametric data from the results of the automated processing (before analyst review). The files in this directory have the prefix *IEB* for initial event bulletin.

IEB.orig

Table A.2 *IEB.orig* Data File

IEB.orig			
attribute name	field no.	Storage type	attribute description
eorid	1	i4	expert system origin id
date	2	date	date (yy mm dd)
time	3	time	time (hr:mm:ss.ms)
lat	4	f4	estimated latitude
lon	5	f4	estimated longitude
depth	6	f4	estimated depth

Table A.2 describes the *IEB.orig* data file. This file gives the event location and origin time determined by the expert system. The link between the expert system origin (*eorid*) and the final analyst-reviewed origin (*forid*) is given in the *ExpSys_Analyst.dbX* data file. All of the attributes in this file were extracted from the origin Version 3 database table at CSS [Anderson et al., 1991]. The attributes have the following definitions:

- eorid:** A unique positive integer which identifies an origin determined by the expert system.
- date:** Date in year-month-day format. This is converted from the Julian date format in the CSS database.
- time:** Event origin time (GMT). This is converted from the epoch time in the CSS database.
- lat:** Estimated event latitude. Latitudes are positive north of the equator.
- lon:** Estimated event longitude. Longitudes are positive east of the Greenwich meridian.
- depth:** Estimated source depth in kilometers. The depths of all events in Data Set #1 were constrained to 0.0 km.

Magnitudes are not calculated for the solutions determined by the expert system. They are calculated after analyst review (see *FEB.orig*).

Table A.3 *IEB.det* Data File

IEB.det			
attribute name	field no.	Storage type	attribute description
eoid	1	i4	expert system origin id
arid	2	i4	arrival id
sta	3	c6	station code
chan	4	c8	channel code
chanid	5	i4	channel id
date	6	date	date (yy mm dd)
time	7	time	time (hr:mm:ss.ms)
iphase	8	c8	reported phase
phase	9	c8	associated phase
amp	10	f4	amplitude (nm)
freq	11	f4	frequency
snr	12	f4	signal-to-noise ratio
velo	13	f4	observed phase velocity
azimuth	14	f4	observed azimuth
fkq	15	i4	f-k quality measure

Table A.3 describes the *IEB.det* data file. This file gives the detection and phase association data determined by the expert system. The attributes in this file were extracted from the **arrival** and **assoc** Version 3 database tables at CSS [Anderson et al., 1991]. The attributes have the following definitions:

- eoid:** A unique positive integer which identifies an origin determined by the expert system.
- arid:** A unique positive integer which identifies an arrival.
- sta:** Code name given to a seismic station. Station codes for NORESS and ARCESS are NRA0 and ARA0, respectively.
- chan:** Code name given to the data channel. Code names for Data Set #1 are *zb* and *hb* for beams formed from data recorded by vertical- and horizontal-component sensors, respectively.
- chanid:** A unique positive integer which identifies the recording channel. For Data Set #1 this is equal to the *IAS* beam number in Table 2.5.
- date:** Date in year-month-day format. This is converted from the Julian date format in the *CSS* database.
- time:** Arrival time (GMT). This is converted from the epoch time in the *CSS* database.

- iphase*: The name initially given to a seismic phase. In Data Set #1 (and in the IAS database at CSS) this is equal to the final phase identification (*phase*, see below) if it is associated with an event. Otherwise, it is the phase name assigned by the expert system during single-station processing. This is discussed in more detail below.
- phase*: Name given to each associated phase (e.g., final phase identification after network processing).
- amp*: This is zero-to-peak displacement amplitude measured on the detecting channel in nanometers. It is corrected for the instrument response at the dominant signal frequency (see *freq* below).
- freq*: Dominant signal frequency in Hertz. This is equal to the reciprocal of the period, *per*, in the CSS Version 3 Database [Anderson et al., 1990].
- snr*: Signal-to-noise ratio measured on the detecting channel. This is equal to the short-term-average amplitude (STAV) divided by the long-term-average amplitude (LTAV) immediately preceding the detection [Bache et al., 1990].
- velo*: Phase velocity estimated using a broadband *f-k* method (km/s). This is equal to the reciprocal of the slowness, *slow*, in the IAS database at CSS.
- azimuth*: Azimuth estimated using a broadband *f-k* method (measured in degrees clockwise from north).
- fkq*: Integer measure of the quality of the *f-k* spectrum. Possible values are 1-4, with the highest quality indicated by *fkq* = 1 [Bache et al., 1990].

The *IEB.det* file includes all detections in a 7-minute window starting 30 s before the theoretical *Pn* arrival time for each event (based on the final origin in *FEB.orig*). This includes phases that are associated with the event, those that are associated with a different event (e.g., mixed events), and those that are not associated with any event. If the detection is not associated with an event, then *eorid* is set to -1.

The possible values for *iphase* in Data Set #1 are *Pn*, *Pg*, *Px*, *P*, *Sn*, *Lg*, *Sx*, *S*, *T*, and *N*. *Px* and *P* are synonyms, as are *Sx* and *S*. These labels are used for *P*- and *S*-type phases for which the path from source to receiver is unknown (e.g., coda detections). The label *T* is assigned to detections with estimated phase velocities > 14 km/s (probable teleseisms). *N* is used if the phase velocity is < 2.8 km/s, or if *fkq* = 4 (probable "noise" detections). The final label assigned to phases that are associated with an event, *phase*, is *Pn*, *Pg*, *Px*, *P*, *Sn*, *Lg*, *Sx*, or *S*. This label is set to "-----" for detections that are not associated with a regional event.

The IAS definitions of *iphase* and *phase* are slightly different than the corresponding IMS definitions because IMS also detects and locates teleseismic events. For example, *P* stands for teleseismic *P* in the IMS database, and it is not synonymous with *Px*. Also, *iphase* is not equal to *phase* for associated detections. Instead, it is equal to the phase label that is assigned during single-station processing.

Table A.4 *IEB.apma* Data File

IEB.apma			
attribute name	field no.	Storage type	attribute description
phase	1	c8	phase
arid	2	i4	arrival id
freq	3	f4	frequency
snr	4	f4	signal-to-noise ratio
amp3	5	f4	3-component amplitude
rect	6	f4	rectilinearity
plan	7	f4	planarity
hvrat	8	f4	horizontal-to-vertical ratio
hmxmn	9	f4	max-to-min horizontal ratio
inang3	10	f4	short-axis incidence angle
azimuth	11	f4	observed azimuth
ema	12	f4	emergence angle
ptime	13	f8	P phase extraction time
stime	14	f8	S phase extraction time
auth	15	c15	author
commid	16	i4	comment id

Table A.4 describes the *IEB.apma* data file. This file gives results from automated particle motion analysis. All attributes in this file were extracted from the *apma* database table at *CSS* which is an *IMS* extension to the Center Version 3 Database [Swanger *et al.*, 1991].

The method used in *IMS* for particle motion analysis was developed by *Jurkevics* [1988]. It computes the polarization ellipse within overlapping time windows by solving the eigenproblem for the covariance matrix. Data from the four 3-component sensors at *NORESS* and *ARCESS* are combined by averaging the individual covariance matrices before solving the eigenproblem. The covariance matrices are computed in the time domain for several frequency bands, and then normalized and averaged to obtain a wide-band estimate for each of the overlapping windows. The *IAS* implementation of this is described by *Bache et al.* [1990].

Several of the particle motion attributes are calculated from the time window with the maximum rectilinearity. These are called *P*-type attributes in the following description. Also, several attributes are calculated from the time window with maximum 3-component amplitude. These are called *S*-type attributes. The particle motion attributes have the following definitions:

phase: Name given to each associated phase. This is currently not filled in the *IAS* database, so it is set to the N/A value of "-" for Data Set #1.

arid: A unique positive integer which identifies an arrival.

freq: Center frequency of the passbands with $snr > 1.5$ used in the averaging. The passbands are 1-2, 2-4, 4-8 and 8-16 Hz. For example, if all bands had $snr > 1.5$, then *freq* would be 8.5 Hz.

snr: Average *snr* for frequency bands that contribute to the final polarization estimates. Each *snr* is the ratio of the maximum signal 3-component amplitude to the maximum pre-arrival noise 3-component amplitude (see *amp3* below).

amp3: Three-component amplitude measured from the time window with maximum rectilinearity (*P*-type attribute). *amp3* is equal to the sum of the square roots of the eigenvalues (e.g., it is the sum of the amplitudes measured along the 3 axes of the polarization ellipsoid). It is called *amp3* in later versions of the *IMS* database.

rect Signal rectilinearity defined as:

$$rect = \left[1 - \frac{\lambda_3 + \lambda_2}{2\lambda_1} \right]^2$$

where λ_1 , λ_2 , and λ_3 are the eigenvalues such that $\lambda_1 > \lambda_2 > \lambda_3$. Later versions of *IMS* use the square root of this quantity. *rect* is a *P*-type attribute.

plan: Signal planarity defined as:

$$plan = \left[1 - \frac{\lambda_3}{\lambda_2} \right]^2$$

Later versions of *IMS* use the square root of this quantity. Planarity is measured from the window with the maximum 3-component amplitude (*S*-type attribute). It is called *plans* in later versions of the *IMS* database.

hvrat: Horizontal to vertical power ratio defined as:

$$hvrat = \frac{c_3 + c_2}{2c_1}$$

where c_1 , c_2 , and c_3 are the diagonal elements of the covariance matrix, and c_1 corresponds to the vertical component. *hvrat* is an *S*-type attribute.

hmxmn: Maximum to minimum horizontal amplitude ratio defined as:

$$hmxmn = \sqrt{\frac{\lambda_1}{\lambda_2}}$$

where λ_1 and λ_2 are the maximum and minimum eigenvalues obtained by solving the 2-D eigensystem using the only the horizontal components. It is an *S*-type attribute.

- inang3***: Incidence angle (measured from the vertical) of the eigenvector associated with the smallest eigenvalue. It is also called the short-axis incidence angle, and it is an *S*-type attribute.
- azimuth***: Azimuth of the eigenvector associated with the largest eigenvalue. It is corrected by 180° to give an estimate of the station-to-event azimuth. *azimuth* is a *P*-type attribute.
- ema***: Apparent incidence angle (measured from the vertical) of the eigenvector associated with the largest eigenvalue. It is also called the long-axis incidence angle, or the emergence angle. It is called *inang1* in later versions of the *IMS* database. It is a *P*-type attribute.
- ptime***: Center of the time window with maximum rectilinearity. All *P*-type attributes are measured from this time window.
- stime***: Center of the time with maximum 3-component amplitude. All *S*-type attributes are measured from this time window.
- auth***: Author. This field is set to the N/A value of "-" for all arrivals in Data Set #1.
- commid***: Comment identification. This attribute is set to the N/A value of -1 for arrivals in Data Set #1.

IEB.sbsnr

Table A.5 *IEB.sbsnr* Data File

IEB.sbsnr			
attribute name	field no.	Storage type	attribute description
arid	1	i4	arrival id
chanid	2	i4	channel id
stav	3	f4	short-term average
ltav	4	f4	long-term average

Table A.5 describes the *IEB.sbsnr* data file. This file gives short-term average signal amplitudes (STAV) and long-term average noise amplitudes (LTAV) on up to six standard beams (these are beams 201, 207, 254, 282, 310, and 312 in Table 2.5). All attributes in this file were extracted from the *sbsnr* database table at CSS which is an *IMS* extension to the Center Version 3 Database [Swanger *et al.*, 1991]. The attributes have the following definitions:

- arid***: A unique positive integer which identifies an arrival.
- chanid***: A unique positive integer which identifies the recording channel. For Data Set #1 this is equal to the *IAS* beam number in Table 2.5.
- stav***: Short-term average signal amplitude in digital counts [Bache *et al.*, 1990].
- ltav***: Long-term average pre-signal amplitude in digital counts [Bache *et al.*, 1990].

The *IEB.sbsnr* table includes the amplitudes on all six beams for detections that are associated with an event. However, only the amplitudes on beam 312 are saved for unassociated detections. Also, there are some cases where all beams could not be formed because of missing or bad data.

Analyst

The *Analyst* directory contains parametric data after review by a seismic analyst. The files in this directory have the prefix *FEB* for final event bulletin.

FEB.orig

Table A.6 *FEB.orig* Data File

FEB.orig			
attribute name	field no.	Storage type	attribute description
forid	1	i4	final origin id
date	2	date	date (yy mm dd)
time	3	time	time (hr:mm:ss.ms)
lat	4	f4	estimated latitude
lon	5	f4	estimated longitude
depth	6	f4	estimated depth
ml	7	f4	local magnitude
nsta	8	i4	No. of recording stations
ndef	9	i4	No. of defining phases

Table A.6 describes the *FEB.orig* data file. This file gives the event location and origin time after analyst review of the expert system solution. The attributes in this file were extracted from the origin Version 3 database table at CSS [Anderson et al., 1991], and the *ev_summary* database table which is an *IMS* extension to the Center Version 3 Database [Swanger et al., 1991].

The first 6 attributes in this file have the same definitions as those described under *IEB.orig* except that the expert system origin identification is replaced with the final origin identification. The other three attributes have the following definitions:

- ml*: Local *Lg* magnitude (see below). magnitude).
- nsta* Number recording stations.
- ndef* Number of defining phases (e.g., phases that are used to constrain the event location).

The local magnitude is referred to as the *IMS* Version 1 *MLg* by Bache et al. [1991]. It is computed from the peak amplitude on a 2–4 Hz incoherent beam in the time window defined by group velocities of 3.0 to 3.6 km/s. It is computed for each array contributing any associated phase to the location solution (i.e., this magnitude is computed even when there is no detected and identified *Lg* phase).

FEB.det

Table A.7 *FEB.det* Data File

FEB.det			
attribute name	field no.	Storage type	attribute description
forid	1	i4	final origin id
arid	2	i4	arrival id
sta	3	c6	station code
chan	4	c8	channel code
chanid	5	i4	channel id
date	6	date	date (yy mm dd)
time	7	time	time (hr:mm:ss.ms)
iphase	8	c8	reported phase
phase	9	c8	associated phase
amp	10	f4	amplitude (nm)
freq	11	f4	frequency
snr	12	f4	signal-to-noise ratio
velo	13	f4	observed phase velocity
azimuth	14	f4	observed azimuth
fkq	15	i4	f-k quality measure

Table A.7 describes the *FEB.det* data file. This file gives the detection and phase association data after analyst review of the automated processing. The attributes in this file were extracted from the arrival and assoc Version 3 database tables at CSS [Anderson et al., 1991].

The attributes in this file have the same definitions as those described under *IEB.det* except that the expert system origin identification is replaced with the final origin identification. Phases that were detected by the automated system appear in both *IEB.det* and *FEB.det* under the same unique arrival identification, *arid*. The only difference between the two files for these detections is that the time and/or phase label may have been changed by the analyst. All other parameters are the same in both files. Phases that are added by an analyst (that were not detected by the automated system) appear only in *FEB.det*. These phases have null values for fields 4–5 and 10–15 since signal processing is not recalled.

FEB.distaz

Table A.8 *FEB.distaz* Data File

FEB.distaz			
attribute name	field no.	Storage type	attribute description
forid	1	i4	final origin id
sta	2	c6	station code
distance	3	f4	epicentral distance (km)
seaz	4	f4	station-to-event azimuth

Table A.8 describes the *FEB.distaz* data file. This file gives the distance and station-to-event azimuth to NORESS and ARCESS for each event in *FEB.orig*. These were calculated from the locations of the center elements of each array, and the event locations in *FEB.orig*.

EVID

The **EVID** directory contains the identification (earthquake or explosion) of each event. This identification is based primarily on a regional seismic bulletin produced by the University of Helsinki [*Sereno*, 1991].

EVID.dbX

Table A.9 *EVID.dbX* Data File

EVID.dbX			
attribute name	field no.	Storage type	attribute description
forid	1	i4	final origin id
evtype	2	c15	event type

Table A.9 describes the *EVID.dbX* data file. This file contains the probable identification of each event in *FEB.orig*. The attributes have the following definitions:

- forid*: A unique positive integer which identifies an origin determined (or validated) by a seismic analyst.
- evtype*: Event type. This is earthquake, mine blast, or explosion (see Section 2.2 of this report). If the event type is followed by "(H)", then the event was identified in the Helsinki Bulletin. Otherwise, the event was identified by *Sereno* [1991].

Helsinki.orig

Table A.10 *Helsinki.orig* Data File

Helsinki.orig			
attribute name	field no.	Storage type	attribute description
forid	1	i4	final origin id
date	2	date	date (yy mm dd)
time	3	time	time (hr:mm:ss.ms)
lat	4	f4	estimated latitude
lon	5	f4	estimated longitude
depth	6	f4	estimated depth
ml	7	f4	local magnitude
evtype	8	c15	event type

Table A.10 describes the *Helsinki.orig* data file. This file contains the origin data from the Helsinki Bulletin for the *IMS* events that were reported in that bulletin. The complete unedited listing from the Helsinki Bulletin is given for each event in *Helsinki.orig.dbX*. Most of the attributes in this table were described previously. The others have the following definitions:

- ml*: Local magnitude from the Helsinki Bulletin. This duration-based magnitude is described by *Wahlström and Ahjos* [1984].
- evtype*: Event type determined by the University of Helsinki. This is either *man-loc* for manual location (these are mining explosions), *earthquake*, or an N/A value of "-----" if the event type was not determined.

MSMP.dbX

Table A.11 *MSMP.dbX* Data File

MSMP.dbX			
attribute name	field no.	Storage type	attribute description
forid	1	i4	final origin id
ml	2	f4	local magnitude
mlp	3	f4	regional P-wave magnitude
mls	4	f4	regional S-wave magnitude
msmp	5	f4	mls - mlp

Table A.11 describes the *MSMP.dbX* data file. This file lists regional *P*-wave magnitudes computed from *P_n* and *P_g* amplitudes, and regional *S*-wave magnitudes computed from *S_n* and *L_g* amplitudes. The difference between them, *msmp*, is a possible discriminant (high values of this difference indicate that the event is an earth-

quake, and low values are inconclusive). The first two attributes are described under *FEB.orig*. The others have the following definitions:

- mlp*: Regional *P*-wave magnitude computed from *P_n* and *P_g* amplitudes [*Bache et al.*, 1991; *IMS Version 2* magnitudes].
- mls*: Regional *S*-wave magnitude computed from *S_n* and *I_g* amplitudes [*Bache et al.*, 1991; *IMS Version 2* magnitudes].
- msmp*: The difference between *mls* and *mlp*.

CEPPKS.dbX

Table A.12 *CEPPKS.dbX* Data File

CEPPKS.dbX			
attribute name	field no.	Storage type	attribute description
for:d	1	i4	final origin id
sta	2	c6	station code
ptyp	3	c6	cepstral peak type code
pkqf	4	f4	cepstral peak quefreny

Table A.12 describes the *CEPPKS.dbX* data file. This file gives the results of cepstral analysis and is useful for identifying ripple-fired mining explosions [*Baumgardt and Zeigler*, 1987]. The first two attributes were described previously. The others have the following definitions:

- ptyp*: Consistent cepstral peak type. This is *FC-PHS* if consistent Fourier cepstral peaks are found across two or more phases for one array, and there is no peak in the noise cepstrum at this quefreny. Otherwise, it is "-" if no consistent cepstral peaks are found.
- pkqf*: Quefreny of the consistent cepstral peak (in seconds). This is set to zero if there are no consistent peaks.

The best evidence for ripple-firing is consistent cepstral peaks across phases and arrays. These are identified in the *CEPPKS.dbX* file as peaks with the same quefreny at both arrays. Cepstral peaks that appear in only one phase at a given station are not reported as consistent peaks, even if there is no peak in the noise cepstrum at that quefreny.

SPVAR.dbX

Table A.13 *SPVAR.dbX* Data File

SPVAR.dbX			
attribute name	field no.	Storage type	attribute description
forid	1	i4	final origin id
arid	2	i4	arrival id
sta	3	c6	station code
phase	4	c8	associated phase
acoef	5	f4	"a" coefficient for non-linear trend
bcoef	6	f4	"b" coefficient for non-linear trend
ccoef	7	f4	"c" coefficient for non-linear trend
fmin	8	f4	min frequency
fmax	9	f4	max frequency
svar	10	f4	variance of detrended log spectrum

Table A.13 describes the *SPVAR.dbX* data file. This file gives the variance of the detrended log spectrum for each phase that is associated with an event. The first four attributes were described previously. The others have the following definitions:

(a,b,c)coef: Three coefficients of the quadratic trend of the log spectrum between frequencies *fmin* and *fmax*.

fmin: Minimum frequency of a band with *snr* > 3 dB.

fmax: Maximum frequency of a band with *snr* > 3 dB.

svar: Variance of the detrended log spectrum between *fmin* and *fmax*.

Array-averaged spectra are computed for a 5-s window starting 0.3 s before each arrival. Noise spectra are calculated for a 5-s window starting 5.3 s before the first arrival. All spectra are corrected for the short-period NORESS/ARCESS instrument response. A log *snr* spectrum is calculated for each detection using the noise before the first arrival. A running mean (width = 0.75 Hz) is applied to this *snr* spectrum, and frequency bands *fmin* to *fmax* are determined such that the smoothed *snr* spectrum is > 3 db (only frequency bandwidths > 4 Hz are retained). A second-order polynomial is fit to the log signal spectra between *fmin* and *fmax* (the coefficients are *acoef*, *bcoef*, and *ccoef*), and this trend is removed. The variance of the detrended log spectrum is calculated and written to the table as *svar*.

Example Data Files

An example of each parametric data file is given in the next few pages for a mining explosion in western USSR.

***** Supply_Analyt.dbl *****

CHASID	FORMID	NOIST	PTIME	SPRING	RESCOUR	AMSD	RTIME
193310	192993	249.002	62.284	2	3	3	2

***** IED.orig *****

CHASID	VR	NR	DO	NR	NR	SS	NS	LAT	LOW	DEPTH
193310	90	02	10	10:13:02.757	59.0000	34.3200	.0000			

***** IED.doc *****

CHASID	ARID	STA	CMAN	CHASID	VR	NR	DO	NR	NR	SS	NS	IPRASE	PIRASE	AMP	FRSQ	SR	VELO	ASIMPTH	0
193310	129350	ARAO	2B	292	90	02	14	10:10:05.332	PG			PG		163.9	6.7	8.50	7.7	154.9	1
-1	129350	ARAO	2B	272	90	02	14	10:10:09.302	PG					61.5	3.3	4.23	7.5	163.11	3
193310	129353	ARAO	2B	275	90	02	14	10:10:24.304	PG			PG		155.0	4.3	10.76	10.9	87.06	1
193310	129360	ARAO	2B	296	90	02	14	10:10:33.902	Lg			Lg		107.5	6.7	4.74	4.6	164.96	2
-1	129364	ARAO	2B	296	90	02	14	10:10:35.059	SK					99.5	10.0	5.24	3.7	251.01	3
-1	129365	ARAO	2B	310	90	02	14	10:20:13.057	SK					954.5	1.2	2.25	6.3	34.05	3
-1	129366	ARAO	2B	301	90	02	14	10:22:01.632	SK					40.2	6.7	4.00	3.2	101.13	3
-1	129367	ARAO	2B	225	90	02	14	10:23:08.107	SK					131.0	4.5	2.46	3.0	176.52	1

***** IED.opma *****

PHASE	ARID	FRSQ	SR	AMP3	RECT	PLAN	HYRAT	MURR	IRANG3	ASIMPTH	SR	PTIME	SR	PTIME	AUTH	CHASID
-	129350	10.0	2.13	1249.2	.504	.160	.72	1.972	87.91	154.57	65.94	90	02	14	10:10:08.345	-1
-	129350	9.1	2.07	2099.2	.470	.111	.940	1.332	55.05	140.07	60.53	90	02	14	10:10:08.505	-1
-	129360	9.1	2.96	3677.2	.540	.22	1.468	1.256	20.89	250.2	70.06	90	02	14	10:10:24.304	-1
-	129364	5.0	1.52	877.5	.834	.126	.377	1.427	70.39	100.25	37.02	90	02	14	10:10:33.902	-1
-	129364	10.0	2.66	1366.2	.200	.066	1.033	1.264	60.37	257.41	65.25	90	02	14	10:10:35.059	-1
-	129365	1.5	1.61	2408.5	.004	.248	.331	1.43	85.64	314.49	60.57	90	02	14	10:20:13.057	-1
-	129366	1.5	1.26	1957.1	.749	.229	.506	2.345	84.71	239.66	60.35	90	02	14	10:22:01.632	-1
-	129367	1.5	1.6	2032.2	.763	.4	1.307	1.302	45.09	316.96	64.77	90	02	14	10:23:08.107	-1

***** IED.abnor *****

ARID	CHASID	STW	STW
129350	201	236.00	161.73
129350	207	45.9	10.79
129350	254	29.30	17.15
129350	202	79.30	12.32
129350	310	626.39	604.35
129350	312	150.32	94.35
129350	312	100.95	90.90
129360	201	192.06	135.14
129360	207	59.76	18.01
129360	254	76.7	23.62
129360	202	76.00	25.72
129360	310	604.23	394.22
129360	312	366.09	116.16
129363	201	82.34	54.27
129363	207	62.33	10.39
129363	254	43.91	26.56
129363	202	140.56	21.1
129363	310	268.35	102.01
129363	312	100.40	152.75
129364	312	295.34	122.92
129365	312	602.09	105.41
129366	312	113.5	103.21
129367	312	110.19	69.26

***** FEB.orig *****

FORID YR MM DD HR:MM:SS.MS LAT LOW DEPTH ML MSTA MDEF
192093 90 02 14 10:16:05.013 61.7003 31.3682 .0000 2.19 2 6

***** FEB.det *****

FORID	ARID STA	CHAN	CHANID	YR	MM	DD	HR:MM:SS.MS	IPHASE	PHASE	AMP	FREQ	SHR	VELD	ALIMUTH O
192093	129358 ARAO	ZB	292	90	02	14	10:18:02.514	Pn	Pn	163.9	6.7	6.58	7.7	154.9 1
-1	129359 ARAO	ZB	272	90	02	14	10:18:09.582	PK	---	61.5	3.3	4.23	7.5	165.11 3
192093	129363 ARAO	ZB	275	90	02	14	10:18:23.871	Pn	Pn	155.8	4.3	10.76	10.9	87.06 1
192093	129360 ARAO	ZB	294	90	02	14	10:19:33.982	Sn	Sn	107.5	6.7	4.74	4.6	164.96 2
-1	129364 ARAO	ZB	296	90	02	14	10:19:35.859	SK	---	99.5	10.0	5.24	3.7	251.01 3
192093	130563 ARAO	-	-1	90	02	14	10:20:04.312	Sn	Sn	-1.0	-1.0	-	-1.0	-
-1	129365 ARAO	ZB	310	90	02	14	10:20:13.857	PK	---	934.5	1.2	2.55	6.3	34.05 3
192093	130562 ARAO	-	-1	90	02	14	10:20:26.051	Lg	Lg	-1.0	-1.0	-	-1.0	-
192093	130564 ARAO	-	-1	90	02	14	10:21:05.305	Lg	Lg	-1.0	-1.0	-	-1.0	-
-1	129366 ARAO	ZB	301	90	02	14	10:22:01.632	SK	---	49.2	6.7	4.88	3.2	181.13 3
-1	129367 ARAO	ZB	225	90	02	14	10:23:08.107	SK	---	131.0	4.5	2.46	3.0	176.52 1

***** FEB.distaz *****

FORID	STA	DISTANCE	SEAZ
192093	ARA0	910.76	160.13
192093	MRA0	1062.64	75.57

***** EVID.db1 *****

FORID Event ID

192093 mine blast (H)

***** Helsinki.orig *****

FORID	YR	MM	DD	HR:MM:SS.MS	LAT	LOW	DEPTH	ML	Event ID
192093	90	02	14	10:16:11.000	61.9000	30.6000	.0000	0.00	manloc-HC13

***** Helsinki.db1 *****

FEB 14, 1990 H= 10 16 11
 LAT= 61.9 N LOW= 30.6 E
 MH USR

***** MSMP.db1 *****

ORID	ML	MLP	MLS	MSMP
192093	2.19	1.9994484	2.3286922	.3292438

***** CEPPES.db1 *****

ORID	STA	PTYP	PROF
192093	ARA0	FC-PHS	.12500057
192093	MRA0	-	0

***** SPVAR.db1 *****

ORID	ARID STA	PHASE	ACOEf	BCOEf	CCOEf	FNIN	FNAX	SVAR
192093	129360 ARAO	Sn	.27733228	-.01924861	.00002419	1.8749917	11.718698	.01240566
192093	130562 ARAO	Lg	.33068138	-.02354399	.00000731	1.8749917	7.2687167	.00759735

DISTRIBUTION LIST

Prof. Thomas Ahrens
Seismological Lab, 252-21
Division of Geological & Planetary Sciences
California Institute of Technology
Pasadena, CA 91125

Prof. Keiiti Aki
Center for Earth Sciences
University of Southern California
University Park
Los Angeles, CA 90089-0741

Prof. Shelton Alexander
Geosciences Department
403 Deike Building
The Pennsylvania State University
University Park, PA 16802

Dr. Ralph Alewine, III
DARPA/NMRO
3701 North Fairfax Drive
Arlington, VA 22203-1714

Prof. Charles B. Archambeau
CIRES
University of Colorado
Boulder, CO 80309

Dr. Thomas C. Bache, Jr.
Science Applications Int'l Corp.
10260 Campus Point Drive
San Diego, CA 92121 (2 copies)

Prof. Muawia Barazangi
Institute for the Study of the Continent
Cornell University
Ithaca, NY 14853

Dr. Jeff Barker
Department of Geological Sciences
State University of New York
at Binghamton
Vestal, NY 13901

Dr. Douglas R. Baumgardt
ENSCO, Inc
5400 Port Royal Road
Springfield, VA 22151-2388

Dr. Susan Beck
Department of Geosciences
Building #77
University of Arizona
Tuscon, AZ 85721

Dr. T.J. Bennett
S-CUBED
A Division of Maxwell Laboratories
11800 Sunrise Valley Drive, Suite 1212
Reston, VA 22091

Dr. Robert Blandford
AFTAC/TT, Center for Seismic Studies
1300 North 17th Street
Suite 1450
Arlington, VA 22209-2308

Dr. G.A. Bollinger
Department of Geological Sciences
Virginia Polytechnical Institute
21044 Derring Hall
Blacksburg, VA 24061

Dr. Stephen Bratt
Center for Seismic Studies
1300 North 17th Street
Suite 1450
Arlington, VA 22209-2308

Dr. Lawrence Burdick
Woodward-Clyde Consultants
566 El Dorado Street
Pasadena, CA 91109-3245

Dr. Robert Burrige
Schlumberger-Doll Research Center
Old Quarry Road
Ridgefield, CT 06877

Dr. Jerry Carter
Center for Seismic Studies
1300 North 17th Street
Suite 1450
Arlington, VA 22209-2308

Dr. Eric Chael
Division 9241
Sandia Laboratory
Albuquerque, NM 87185

Prof. Vernon F. Cormier
Department of Geology & Geophysics
U-45, Room 207
University of Connecticut
Storrs, CT 06268

Prof. Steven Day
Department of Geological Sciences
San Diego State University
San Diego, CA 92182

Marvin Denny
U.S. Department of Energy
Office of Arms Control
Washington, DC 20585

Dr. Cliff Frolich
Institute of Geophysics
8701 North Mopac
Austin, TX 78759

Dr. Zoltan Der
ENSCO, Inc.
5400 Port Royal Road
Springfield, VA 22151-2388

Dr. Holly Given
IGPP, A-025
Scripps Institute of Oceanography
University of California, San Diego
La Jolla, CA 92093

Prof. Adam Dziewonski
Hoffman Laboratory, Harvard University
Dept. of Earth Atmos. & Planetary Sciences
20 Oxford Street
Cambridge, MA 02138

Dr. Jeffrey W. Given
SAIC
10260 Campus Point Drive
San Diego, CA 92121

Prof. John Ebel
Department of Geology & Geophysics
Boston College
Chestnut Hill, MA 02167

Dr. Dale Glover
Defense Intelligence Agency
ATTN: ODT-1B
Washington, DC 20301

Eric Fielding
SNEE Hall
INSTOC
Cornell University
Ithaca, NY 14853

Dr. Indra Gupta
Teledyne Geotech
314 Montgomery Street
Alexandria, VA 22314

Dr. Mark D. Fisk
Mission Research Corporation
735 State Street
P.O. Drawer 719
Santa Barbara, CA 93102

Dan N. Hagedorn
Pacific Northwest Laboratories
Battelle Boulevard
Richland, WA 99352

Prof Stanley Flatte
Applied Sciences Building
University of California, Santa Cruz
Santa Cruz, CA 95064

Dr. James Hannon
Lawrence Livermore National Laboratory
P.O. Box 808
L-205
Livermore, CA 94550

Dr. John Foley
NER-Geo Sciences
1100 Crown Colony Drive
Quincy, MA 02169

Dr. Roger Hansen
HQ AFTAC/TTR
Patrick AFB, FL 32925-6001

Prof. Donald Forsyth
Department of Geological Sciences
Brown University
Providence, RI 02912

Prof. David G. Harkrider
Seismological Laboratory
Division of Geological & Planetary Sciences
California Institute of Technology
Pasadena, CA 91125

Dr. Art Frankel
U.S. Geological Survey
922 National Center
Reston, VA 22092

Prof. Danny Harvey
CIRES
University of Colorado
Boulder, CO 80309

Prof. Donald V. Helmberger
Seismological Laboratory
Division of Geological & Planetary Sciences
California Institute of Technology
Pasadena, CA 91125

Prof. Eugene Herrin
Institute for the Study of Earth and Man
Geophysical Laboratory
Southern Methodist University
Dallas, TX 75275

Prof. Robert B. Herrmann
Department of Earth & Atmospheric Sciences
St. Louis University
St. Louis, MO 63156

Prof. Lane R. Johnson
Seismographic Station
University of California
Berkeley, CA 94720

Prof. Thomas H. Jordan
Department of Earth, Atmospheric &
Planetary Sciences
Massachusetts Institute of Technology
Cambridge, MA 02139

Prof. Alan Kafka
Department of Geology & Geophysics
Boston College
Chestnut Hill, MA 02167

Robert C. Kemerait
ENSCO, Inc.
445 Pineda Court
Melbourne, FL 32940

Dr. Max Koontz
U.S. Dept. of Energy/DP 5
Forrestal Building
1000 Independence Avenue
Washington, DC 20585

Dr. Richard LaCoss
MIT Lincoln Laboratory, M-200B
P.O. Box 73
Lexington, MA 02173-0073

Dr. Fred K. Lamb
University of Illinois at Urbana-Champaign
Department of Physics
1110 West Green Street
Urbana, IL 61801

Prof. Charles A. Langston
Geosciences Department
403 Deike Building
The Pennsylvania State University
University Park, PA 16802

Jim Lawson, Chief Geophysicist
Oklahoma Geological Survey
Oklahoma Geophysical Observatory
P.O. Box 8
Leonard, OK 74043-0008

Prof. Thorne Lay
Institute of Tectonics
Earth Science Board
University of California, Santa Cruz
Santa Cruz, CA 95064

Dr. William Leith
U.S. Geological Survey
Mail Stop 928
Reston, VA 22092

Mr. James F. Lewkowicz
Phillips Laboratory/GPEH
Hanscom AFB, MA 01731-5000(2 copies)

Mr. Alfred Lieberman
ACDA/VI-OA State Department Building
Room 5726
320-21st Street, NW
Washington, DC 20451

Prof. L. Timothy Long
School of Geophysical Sciences
Georgia Institute of Technology
Atlanta, GA 30332

Dr. Randolph Martin, III
New England Research, Inc.
76 Olcott Drive
White River Junction, VT 05001

Dr. Robert Masse
Denver Federal Building
Box 25046, Mail Stop 967
Denver, CO 80225

Dr. Gary McCartor
Department of Physics
Southern Methodist University
Dallas, TX 75275

Prof. Thomas V. McEvilly
Seismographic Station
University of California
Berkeley, CA 94720

Dr. Art McGarr
U.S. Geological Survey
Mail Stop 977
U.S. Geological Survey
Menlo Park, CA 94025

Dr. Keith L. McLaughlin
S-CUBED
A Division of Maxwell Laboratory
P.O. Box 1620
La Jolla, CA 92038-1620

Stephen Miller & Dr. Alexander Florence
SRI International
333 Ravenswood Avenue
Box AF 116
Menlo Park, CA 94025-3493

Prof. Bernard Minster
IGPP, A-025
Scripps Institute of Oceanography
University of California, San Diego
La Jolla, CA 92093

Prof. Brian J. Mitchell
Department of Earth & Atmospheric Sciences
St. Louis University
St. Louis, MO 63156

Mr. Jack Murphy
S-CUBED
A Division of Maxwell Laboratory
11800 Sunrise Valley Drive, Suite 1212
Reston, VA 22091 (2 Copies)

Dr. Keith K. Nakanishi
Lawrence Livermore National Laboratory
L-025
P.O. Box 808
Livermore, CA 94550

Dr. Carl Newton
Los Alamos National Laboratory
P.O. Box 1663
Mail Stop C335, Group ESS-3
Los Alamos, NM 87545

Dr. Bao Nguyen
HQ AFTAC/TTR
Patrick AFB, FL 32925-6001

Prof. John A. Orcutt
IGPP, A-025
Scripps Institute of Oceanography
University of California, San Diego
La Jolla, CA 92093

Prof. Jeffrey Park
Kline Geology Laboratory
P.O. Box 6666
New Haven, CT 06511-8130

Dr. Howard Patton
Lawrence Livermore National Laboratory
L-025
P.O. Box 808
Livermore, CA 94550

Dr. Frank Pilotte
HQ AFTAC/TT
Patrick AFB, FL 32925-6001

Dr. Jay J. Pulli
Radix Systems, Inc.
2 Taft Court, Suite 203
Rockville, MD 20850

Dr. Robert Reinke
ATTN: FCTVTD
Field Command
Defense Nuclear Agency
Kirtland AFB, NM 87115

Prof. Paul G. Richards
Lamont-Doherty Geological Observatory
of Columbia University
Palisades, NY 10964

Mr. Wilmer Rivers
Teledyne Geotech
314 Montgomery Street
Alexandria, VA 22314

Dr. George Rothe
HQ AFTAC/TTR
Patrick AFB, FL 32925-6001

Dr. Alan S. Ryall, Jr.
DARPA/NMRO
3701 North Fairfax Drive
Arlington, VA 22209-1714

Dr. Richard Sailor
TASC, Inc.
55 Walkers Brook Drive
Reading, MA 01867

Prof. Charles G. Sammis
Center for Earth Sciences
University of Southern California
University Park
Los Angeles, CA 90089-0741

Prof. Christopher H. Scholz
Lamont-Doherty Geological Observatory
of Columbia University
Palisades, CA 10964

Dr. Susan Schwartz
Institute of Tectonics
1156 High Street
Santa Cruz, CA 95064

Secretary of the Air Force
(SAFRD)
Washington, DC 20330

Office of the Secretary of Defense
DDR&E
Washington, DC 20330

Thomas J. Sereno, Jr.
Science Application Int'l Corp.
10260 Campus Point Drive
San Diego, CA 92121

Dr. Michael Shore
Defense Nuclear Agency/SPSS
6801 Telegraph Road
Alexandria, VA 22310

Dr. Matthew Sibol
Virginia Tech
Seismological Observatory
4044 Derring Hall
Blacksburg, VA 24061-0420

Prof. David G. Simpson
IRIS, Inc.
1616 North Fort Myer Drive
Suite 1440
Arlington, VA 22209

Donald L. Springer
Lawrence Livermore National Laboratory
L-025
P.O. Box 808
Livermore, CA 94550

Dr. Jeffrey Stevens
S-CUBED
A Division of Maxwell Laboratory
P.O. Box 1620
La Jolla, CA 92038-1620

Lt. Col. Jim Stobie
ATTN: AFOSR/NL
Bolling AFB
Washington, DC 20332-6448

Prof. Brian Stump
Institute for the Study of Earth & Man
Geophysical Laboratory
Southern Methodist University
Dallas, TX 75275

Prof. Jeremiah Sullivan
University of Illinois at Urbana-Champaign
Department of Physics
1110 West Green Street
Urbana, IL 61801

Prof. L. Sykes
Lamont-Doherty Geological Observatory
of Columbia University
Palisades, NY 10964

Dr. David Taylor
ENSCO, Inc.
445 Pineda Court
Melbourne, FL 32940

Dr. Steven R. Taylor
Los Alamos National Laboratory
P.O. Box 1663
Mail Stop C335
Los Alamos, NM 87545

Prof. Clifford Thurber
University of Wisconsin-Madison
Department of Geology & Geophysics
1215 West Dayton Street
Madison, WS 53706

Prof. M. Nafi Toksoz
Earth Resources Lab
Massachusetts Institute of Technology
42 Carleton Street
Cambridge, MA 02142

Dr. Larry Turnbull
CIA-OSWR/NED
Washington, DC 20505

DARPA/RMO/SECURITY OFFICE
3701 North Fairfax Drive
Arlington, VA 22203-1714

Dr. Gregory van der Vink
IRIS, Inc.
1616 North Fort Myer Drive
Suite 1440
Arlington, VA 22209

HQ DNA
ATTN: Technical Library
Washington, DC 20305

Dr. Karl Veith
EG&G
5211 Auth Road
Suite 240
Suitland, MD 20746

Defense Intelligence Agency
Directorate for Scientific & Technical Intelligence
ATTN: DTIB
Washington, DC 20340-6158

Prof. Terry C. Wallace
Department of Geosciences
Building #77
University of Arizona
Tuscon, AZ 85721

Defense Technical Information Center
Cameron Station
Alexandria, VA 22314 (2 Copies)

Dr. Thomas Weaver
Los Alamos National Laboratory
P.O. Box 1663
Mail Stop C335
Los Alamos, NM 87545

TACTEC
Battelle Memorial Institute
505 King Avenue
Columbus, OH 43201 (Final Report)

Dr. William Wortman
Mission Research Corporation
8560 Cinderbed Road
Suite 700
Newington, VA 22122

Phillips Laboratory
ATTN: XPG
Hanscom AFB, MA 01731-5000

Prof. Francis T. Wu
Department of Geological Sciences
State University of New York
at Binghamton
Vestal, NY 13901

Phillips Laboratory
ATTN: GPE
Hanscom AFB, MA 01731-5000

AFTAC/CA
(STINFO)
Patrick AFB, FL 32925-6001

Phillips Laboratory
ATTN: TSML
Hanscom AFB, MA 01731-5000

DARPA/PM
3701 North Fairfax Drive
Arlington, VA 22203-1714

Phillips Laboratory
ATTN: SUL
Kirtland, NM 87117 (2 copies)

DARPA/RMO/RETRIEVAL
3701 North Fairfax Drive
Arlington, VA 22203-1714

Dr. Michel Bouchon
I.R.I.G.M.-B.P. 68
38402 St. Martin D'Herès
Cedex, FRANCE

Dr. Michel Campillo
Observatoire de Grenoble
I.R.I.G.M.-B.P. 53
38041 Grenoble, FRANCE

Dr. Jorg Schlittenhardt
Federal Institute for Geosciences & Nat'l Res.
Postfach 510153
D-3000 Hannover 51, GERMANY

Dr. Kin Yip Chun
Geophysics Division
Physics Department
University of Toronto
Ontario, CANADA

Dr. Johannes Schweitzer
Institute of Geophysics
Ruhr University/Bochum
P.O. Box 1102148
4360 Bochum 1, GERMANY

Prof. Hans-Peter Harjes
Institute for Geophysic
Ruhr University/Bochum
P.O. Box 102148
4630 Bochum 1, GERMANY

Commander and Director
USAE Waterways Experiment Station
Attn: CEWES-IM-MI-R
Alfrieda S. Clark, CD Dept/0597
3909 Halls Ferry Road
Vicksburg, MS 39180-6199

Prof. Eystein Husebye
NTNF/NORSAR
P.O. Box 51
N-2007 Kjeller, NORWAY

David Jepsen
Acting Head, Nuclear Monitoring Section
Bureau of Mineral Resources
Geology and Geophysics
G.P.O. Box 378, Canberra, AUSTRALIA

Ms. Eva Johannisson
Senior Research Officer
National Defense Research Inst.
P.O. Box 27322
S-102 54 Stockholm, SWEDEN

Dr. Peter Marshall
Procurement Executive
Ministry of Defense
Blacknest, Brimpton
Reading FG7-FRS, UNITED KINGDOM

Dr. Bernard Massinon, Dr. Pierre Mechler
Societe Radiomana
27 rue Claude Bernard
75005 Paris, FRANCE (2 Copies)

Dr. Svein Mykkeltveit
NTNT/NORSAR
P.O. Box 51
N-2007 Kjeller, NORWAY (3 Copies)

Prof. Keith Priestley
University of Cambridge
Bullard Labs, Dept. of Earth Sciences
Madingley Rise, Madingley Road
Cambridge CB3 0EZ, ENGLAND